The variety of forced atmospheric structure in response to tropical SST anomaly found in APE results

Kensuke NAKAJIMA

Faculty of Sciences, Kyushu University, Fukuoka, Japan

and

Yukiko YAMADA

Faculty of Sciences, Hokkaido University, Sapporo, Japan

and

Yoshiyuki O. TAKAHASHI

Center for Planetary Sciences, Kobe, Japan
Kobe University, Kobe, Japan

and

Masaki ISHIWATARI

Faculty of Sciences, Hokkaido University, Sapporo, Japan

and

Wataru OHFUCHI

Earth Simulator Center, Japan Agency of Marine Science and Technology, Yokohama, Japan

and

Yoshi-Yuki HAYASHI

Center for Planetary Sciences, Kobe, Japan
Kobe University, Kobe, Japan

October 31, 2011

Corresponding author: Kensuke Nakajima, Faculty of Sciences, Kyushu University, 6-10-1, Hakozaki, Fukuoka, Fukuoka 812-8581, Japan.
E-mail: kensuke@geo.kyushu-u.ac.jp

Abstract

The variety of precipitation and circulation structures that appear in the numerical experiments conducted in the Aqua Planet Experiment Project in response to equatorial SST anomaly are compared. For a localized equatrial warm SST anomaly of 3KEQ, in all of the models, precipitation increases over the localized SST anomaly. However, the intensity of the precipitation response is found to vary considerably among the models. The difference of precipitation intensity realized in the un-perturbed, zonally symmetric SST in the corresponding models partly explains the variety of the intensity of the precpitation anomaly averaged in tropical latitudes. The vertical structure of the circulation responding to the precipitation anomaly differ considerably among the models, presumably resulting mainly from the different specifications of convective parameterizations. The horizontal structure of the circulation response, where common feature can be identified, is characterized by the Rossby waves which develop mainly eastward from the SST anomaly. Rossby response to the west and Kelvin response to the east of the SST anomaly expected from the standard Matsuno-Gill equatorial response theory are absent or obscured. The intensity of the extratropical response also varies significantly among the models, which can be explained, to some degree, by the variety of the tropical rainfall response intensity. The apparent departure from the framework of tropical response of Matsuno(1966)

or Gill(1980) results from the weak absolute vorticity gradient and strong westerly in the tropical upper troposphere realized in the series of experiments in APE employing the CONTROL SST as the "basic state" SST distribution. It is demonstrated that circulation feature more similar to the Matsuno-Gill theory develops in a supplimental experiment that examines the response to a localized equatorial SST anomaly employing the FLAT SST profile of APE as the "basic state" SST distribution. The mechanism of the different response that develop in the 3KEQ experiments and the supplemental experiment are interpreted in the framework of Rossby wave source discussed by Sardeshmukh and Hoskins(1988).

The response to the wavenumber one variation of the equatorial SST of 3KW1 cases are described only briefly. The equatorial precipitation response is characterized largely with the wavenumber one longitudinal variation, which is shifted to the west of the SST variation by around 30 degrees. The intensity of the response near the equator varies considerably, being partly explained by the degree of concentration of the ITCZ rainfall in the corresponding CONTROL expeiments. The intensity of the precpitation anomaly averaged in tropical latitudes strongly correlated with the anomaly of latent heat flux from the surface. As in the cases with the localized SST anomaly, the vertical structure of the circulation responding to the precipitation anomaly differ considerably among the models. The

horizontal structure of the circulation response, where common feature can again be identified, is characterized by wavenumber one Rossby response in the subtropics and mid-latitudes; the former is baroclinic and the latter is barotropic. Significant acceleration of zonal mean zonal wind can be found in most models. The magnitude of the acceleration does not correlate with the intensity of precipittion response; Analysis of Rossby wave source implies the presence of off-equatorial precipitation anomaly is important for the structure of Rossby response that would transport zonal momentum to the equator.

1. Introduction

The general circulation of the earth's atmosphere is driven by thermal inhomogeneity in itself or of the ground or oceanic surface below. The thermal inhomogeneity originates primarity from the meridional inhomogeneity of solar radation resulting from the spherical geometry of the earth, so that the contrast dominates in the meridional direction, resulting in Hadley circulation (Held and Hou 1980). However, in addition to the planetary scale meridional thermal contrast, there is zonal contrast of surface inhomogeneity caused by the land-sea contrast and various types of zonal thermal contrast of sea surface temperature (SST). Such thermal contrast drives a variety of zonally inhomogeneous response in the atmosphere (Webster, 1983), such as inhomogeneity of precipitation (Lindzen and Nigam, 1987; Neelin and Held, 1987), zonally propagating equatorial waves (Matsuno, 1966; Gill, 1980), and Rossby wave train propagating to extratropics (Bjerkness, 1969; Hoskins and Karoly, 1981). The precipitation response are not only directly forced by the surface condition but also caused as long distance effect of remote anomalies (Hosaka et al, 1998; Nakajima et al, 2004) These atmospheric response, in return, affects the condition of the ground and sea surface below, all of which consist of a mutually feedback system of land-sea-atmosphere system. Appropriate understanding of such interaction is not only important in theoretical interest but also indispens-

able for practical purpose such as weather prediction and the projection of future climate.

Bearing such importance of the zonal inhomogeneity of SST in mind, the Aqua Planet Experiment Project (APE) defined, in addition to five zonally symmetric SST distributions, three zonally inhomogeneous SST distributions to be specified in the AGCM intercomparison. As is presented in Neale and Hoskins (2000a) and reprocuded in Blackburn and Hoskins (2011) in this special issue, each of these three distributions, 1KEQ, 3KEQ, 3KW1, consists of anomaly of SST placed near the equator superposed on a zonally homoneteous SST distrubution. In the two of them, 1KEQ and 3KEQ, the SST anomaly is localized, whereas in the other, 3KW1, the SST anomaly takes a form of zonal wavenumber one variation. The purpose of these specifications are, as stated in Blackburn and Hoskins (2011), (i) to determine the circulation response to a localised anomaly in tropical SST, what process determine the local and grobal responses, and how these vary between models, and (ii) to determine the circulation response to a planetary scale anomaly in tropical SST, which involves the generation and propagation of planetary-scale Rossby waves, their longitudinal modulation of the extra-tropical storm-track and their impact on meridional transports. All of these issues are among the important ring of chains stranding the complex behavior of atmosphere in the climate system.

This paper decribes and compares the structure of response to the zonal inhomogeneous SST anomaly realized in 18 AGCM runs conducted by 15 participating groups of the APE. We focus mainly on the steady state tropical response of precipitation which, we expected, is the primary "conduit" from the tropical SST to the global atmosphere. The extratropical dynamical response are only briefly touched; the behavior of storm track are left entirely for a future research.

As is shown later, the structure of the response to the localized SST anomaly is disctinctly different from the classical shallow water equatorial beta plane response of Matsuno(1966) and Gill(1980). Although this character has been already found in Neale and Hoskins (2000b), the departure from Matsuno-Gill pattern is not a trivial issue but requires explanation; at least in one aqua planet AGCM experiment (Hosaka et al. 1998), the response similar to Matsuno-Gill pattern is obtained. To resolve this controversy, we present the result of a supplimentary pair of experiments but with different specification of basic SST distribution, where the response is fairly similar to Matsuno-Gill pattern. We will compare these case and one of the runs with 3KEQ SST of APE examining the Rossby wave sources (Sardeshmukh and Hoskins 1988).

The paper is organized as follows. Section 2 will explain the setup of experiment and method of analysis. In Section 3 and Section 4, response to

a localised equatorial SST anomaly and zonal wavenumber one variation of SST will be exained, respectively. Excitaion mechanism of the large scale response will be discussed in Section 5. Concluding remarks will be given in the last section.

2. Methods

2.1 Specification of SST

Source data of the present article is the results of aqua planet AGCM runs with CONTROL, 3KEQ, and 3KW1 SST distributions of the APE project conducted by 15 participating groups, whose specifications are briefly summarized in Table 1. For details, readers are referred to the APE-ATLAS (Williamson et al. 2011) or Blackburn and Hoskins (2011). There are several exception from the standard specification in these experiments, which are: (i) the longitudinal location of the SST anomaly in LASG is 90 degrees to the east of the location used in other models, (ii) the mean surface pressure in GFDL is 1000hPa instead of the standard value of 101325Pa, and, (iii) the western half of the SST anomaly is lacking in 1KEQ and 3KEQ experiment of EC05. The points (ii) and (iii) above should affect the characteristics of the response to the SST anomaly, which should be born in mind in strict intercomparison. We judge that these models are worth presented

because these models display, as will be shown below, unique character of response, and enrich the variety of the models to be compared. Table 1

In CONTROL experiments, the SST [1] is zonally uniform and given as

$$T_{\mathrm{CONTROL}}(\lambda,\varphi)=\begin{cases} 27\left[1-\sin^2\left(\frac{90}{60}\varphi\right)\right] & \text{if } |\varphi|<60, \\ 0 & \text{if } |\varphi|\geq 60. \end{cases} \tag{1}$$

In 1KEQ, 3KEQ, and 3KW1 experiments, the anomalies are added to the CONTROL SST given above, which are

$$T_{\mathrm{1KEQ}}(\lambda,\varphi)=\begin{cases} \cos^2\left(\frac{90}{15}\varphi\right)\cos^2\left(\frac{90}{30}\lambda\right) & \text{if } |\varphi|<15 \text{ and } |\lambda|<30, \\ 0 & \text{otherwise,} \end{cases} \tag{2}$$

$$T_{\mathrm{3KEQ}}(\lambda,\varphi)=\begin{cases} 3\cos^2\left(\frac{90}{15}\varphi\right)\cos^2\left(\frac{90}{30}\lambda|\right) & \text{if } |\varphi|<15 \text{ and } |\lambda|<30, \\ 0 & \text{otherwise,} \end{cases} \tag{3}$$

and

$$T_{\mathrm{3KW1}}(\lambda,\varphi)=\begin{cases} 3\cos^2\left(\frac{90}{30}\varphi\right)\sin(\lambda) & \text{if } |\varphi|<30, \\ 0 & \text{otherwise.} \end{cases} \tag{4}$$

By comparing 1KEQ or 3KEQ with CONTROL, we can examine the response of the global atmosphere to a localized equatorial SST anomaly, including anomalous precipitation and equatorial and extratropical waves activities which follow. By comparison between 1KEQ and 3KEQ, we can obtain a hint on how 'linearly' the atmosphere behave to the imposed SST

[1] The SST in this section is given in Celsius degree.

anomaly. Comparison between 3KW1 and CONTROL should provide information on atmospheric response to planetary scale zonal variation of tropical SST.

The CONTROL SST distribution differ from the climatological SST distribution at least in the following two aspects, which are, (1)sharper SST gradient prevails over the lower latitudes, and (2) high latitude regions are covered with uniform SST. Because of these difference of meridional SST distributions and the absense of zonal land-sea contrasts in addition, the polar jet and the subtropical jet in the CONTROL experiments are merged and constitutes a very strong jet situated around 30 degrees latitudes. as is presented in Blackburn et al(2011) and Williamson et al (2011). Due to the equatorward shift and the strength of the jets, the response of the atmosphere to the equatorial SST anomaly seems to be peculiar to some extent as will be shown later. Therefore, to place the APE cases in broader context, we also present a supplementary pair of experiments with the FLAT SST of APE project written below and FLAT3KEQ SST, which is the superposition of the FLAT SST and the 3KEQ SST anomaly defined above.

$$T_{\mathrm{FLAT}}(\lambda,\varphi) = \begin{cases} 27\left[1-\sin^4\left(\frac{90}{60}\varphi\right)\right] & \text{if } |\varphi| < 60 \\ 0 & \text{if } |\varphi| \geq 60 \end{cases} \tag{5}$$

The supplemental pair of experiments are conducted using a modified version of AGUforAPE model, in which a prognostic Arakawa Schubert scheme

(Pan and Randall 1998) is employed as cumulus parameterization instead of the original one (Emanuel and Zivkovic-Rothman 1999). This choice is mainly for presentation purpose. Detail will be explained later.

2.2 Analysis

Most of the material presented in this paper concerns the steady response of variables in AGCMs to the anomaly of SST defined above; we leave examination of all kinds of time dependent response, including the response of convectively coupled equatorial waves, the change of transport properties of mid-latitude baroclinic waves, or the process of development of stationary waves, for future research.

The steady response of particular variable is calculated by subtracting time mean zonal mean of the variables in CONTROL experiment from time-mean field of the variable in the experiment with corresponding SST anomaly introduced (1KEQ, 3KEQ, or 3KW1). For the supplemental pair of experiments employing FLAT SST as the "basic state" SST, the response is calculated by subtracting time mean zonal mean of the variables in FLAT experiment from time-mean field of the variable in the experiment with corresponding SST anomaly introduced (FLAT3KEQ).

In order to investigave the exitation mechanism of wave component in the response field, the Rossby wave source terms discussed by Sardeshmukh

and Hoskins (1988) is diagnosed for the stationary component of the response. They are defined in the barotropic vorticity equation

$$\left(\frac{\partial}{\partial t} + \mathbf{v}_\psi \cdot \nabla\right)\zeta = S_{ad} + S_{div}, \tag{6}$$

where S_{ad} and S_{div} are the advective and divergent source of vorticity, respectively, and defined as

$$S_{ad} \equiv -\mathbf{v}_\chi \cdot \nabla\zeta, \tag{7}$$

$$S_{div} \equiv -\zeta D, \tag{8}$$

where ζ is absolute vorticity, D is divergence; $\mathbf{v}_\chi$ and $\mathbf{v}_\psi$ are divergent and rotational component of wind, respectively.

S_{ad} and S_{div} are calculated by the following procedure: First, ζ and D are calculated from the time mean wind field. Second, stream function, Ψ, and velocity potential, χ, are obtained from vorticity and divergence, respectively. The inversion of spherical Laplacian operator is conducted employing the spectral method. Third, rotational and divergent components of wind vectors are obtained by differentiating the stream function and velocity potential, respectively. Forth, advective and divergent source terms are calulated by using thus obtained divergent wind vector and vorticity.

3. Response to a localized equatorial SST anomaly

3.1 Precipitation response

Time mean precipitation anomaly in 15 AGCM runs in 3KEQ case are shown Fig. 1. In all of the models, precipitation increases over the localized SST anomaly. However, the intensity and size are considerably model dependent. The latitudinal structure seems to be related to the original latitudinal structure of precipitation of the CONTROL experiment in the corresponding models. In particular, the precipitation response on the SST anomaly tends to have a single peak at the equator in the models where the ITCZ is single peaked (AGUforAPE, CSIROold, DWD, ECMWF05, GFDL, LASG, MIT, MRI, and UKMOn96), whereas there are two peaks of anomaly located north and south of the equator in the models where the ITCZ is double peaked (CGAM, AGUforAPE, CSIROstd, ECMWF07, K1JAPAN, and NCAR). GSFC seems to be an exception; the anomaly has a clear peak at the equator in spite that the ITCZ in CONTROL experiment is double peaked. However, this might be reasonable because the split of the double ITCZ in the CONTROL experiment is not very clear.

Other than the distinct and localized positive anomaly directly above the SST anomaly, there are at least two types of remote response of precipitation. One is negative anomaly of precipitation generally ditributeded

along the equator in most of the models. As do the positive anomaly over the SSTA, the structure of the negative anomaly vary among the models. Another is a north-south symmetric signal along the mid-latitude baroclinic zone; precipitation increase at 40–70 degrees to the east of the SSTA in most of the models, whereas negative anomaly can be found in several models around the longitudes at which the SSTA is placed. The positive anomaly in the mid-latitudes may be considered as a generic structure of the increase of rainfall observed in the western United States during the time of El Nino (Hoerling and Kumar 2002). The mid-latitude precipitation response is acompanied with pressure anomaly as will be described later.

More closely examining the remote response along the equator, we find that subtle feature superposed on the general negative trend. First, the reduction of precipitation has latitudinal structure, which is model dependent. The latitudinal structure in each of the models, somewhat similar to the case with the positive precipitation anomaly above the SST anomaly, largely reflects the structure of ITCZ in unperturbed (CONTROL) experiment in the corresponding model; the latitudinal structure of intensity of the rainfall reduction is, in large, the "negative" image of the rainfall intensity of ITCZ in CONTROL experiments. This does not seem to be unnatural because precipitation can not reduce much at the location of small amount

of rainfall from the beginning. Even keeping this factor in mind, however, there is a tendency that is commonly notable in many models: the remote equatorial precipitation tends to be enhanced (or less suppressed) just at the equator and suppressed at the latitudes off-equator. This is clearly noted especially in the models with double ITCZ in CONTROL (e.g., CGAM, ECMWF07, K1JAPAN, NCAR and UKMOn96). This tendency reminds us of the equatorial precipitation enhancement found in the response to an localized equatorial SST anomaly in previous studies (Hosaka et al, 1998), and may be interpreted as the equatorial Kelvin wave response. We will return to this issue later in section 5.

Second, the reduction of precipitation is not zonally uniform. Most notable is that, in most of the models, the negative anomaly is most intense to the west of the SST anomaly; the magnitude of the reduction reaches as much as one-forth of that of the positive anomaly over the SSTA in some models. The area of intense decrease of precpitaion extends zonally over 5,000 km. An exceptions is CGAM, in which the signature of precipitation anomaly is positive along equator to the west of SSTA, which may be explained as the equatorial enhancement of precipitation noted above. Similar significant reduction of precipitation anomaly to the west of SST anomaly is found in previous studies (Hosaka et al, 1998; Neale and Hoskins,2000b) and has been explained as a result of Rossby response. We will also re-

turn to this issue later in section 5. In addition to the intense reduction to the west of the SSTA, weak wavelike variation having typical wavelength of 7000km can be noted with varying amplitude in different models. This feature may well be related to the extratropical dynamical signature that will be discussed shortly below. Fig. 1

3.2 Horizontal structure of Response

Horizontal structure of the response, namely anomalies of horizontal wind and geopotential height, on the 250hPa and 850hPa surface in all models are shown in figure 2 and 3, respectively. At a glance, considerable degree of variety among the response in different models is recognized. However, we try to identify features common in the models before considering the variety.

The feature most easily recognized in common is a north-south symmetric pair of barotropic Rossby wave trains. Typically, they emerge as the pair of anticylones at $(\lambda, \varphi) = (10°, \pm 30°)$, propagate to higher latitudes form the pair of cyclones at $(\lambda, \varphi) = (50°, \pm 40°)$, then turns back to lower latitude as the pair of anticyclones at $(\lambda, \varphi) = (90°, \pm 30°)$, precice location of the cyclonic/anticyclonic centers differing in the different models; further downstream development can be traced in some models. As will be shown later, the Rossby wave train is forced by the northward/southward

wind anomaly diverging from the location of positive precipitation anomaly above the SST anomaly.

Another type of feature that is noted in many of the models is more or less sinusoidal wave feature along the $\pm 30^\circ$ latitude circle. This feature is similar to the wavenumber 5 quasi-stationary feature noticed in the CONTROL experiments (Blackburn et al,2011; Williamson et al, 2011), and, figures 1, 2 and 3 compared, seems to be affecting the equatorial precipitation as is demonstrated in Zappa et al (2011). The existence of similar stationary wavelike variation in CONTROL cases could imply that the wavelike variation found in the 3kEQ experiments is merely noise. Nevertheless, if the phase of the wavy variation is locked to the SST anomaly, this feature should be regarded as significant signal.T There are at least two pices of evidence supporting this possiblity: the amplitude of the variation is larger in 3KEQ than in CONTROL by a factor of about 2 to 3 in some models, and, distinct north-south symmetry is noted in the cases where this signal is strong whereas such clear symmetry is not necessarily found in CONTROL cases (see fig.4.99 of Willamson et al, 2011). More detailed analysis is required to clarify this issue.

The fact that we can recognize in most of the models is that, rather puzzlingly, equatorial Kelvin signal to the east and equatorial Rossby signal to the west of the SST anomaly, which could be expected to emerge

based on the standard theory of the thermal response of tropical atmosphere (Matsuno, 1966; Gill, 1980), are not immediately identified in most models. Actually, anything similar to typical equatorial wave response can be identified only in two of the models, CSIROold and MIT, where zonal convergent(divergent) flow along the equator can be noted in lower (upper) troposphere. In other models, baroclinic response of zonal flow is almost absent at the equator in the zonal interval between the center of SST anomaly and $\sim$ 50 degrees longitude. Namely, in CSIROstd, ECMWF07, GFDL, K1JAPAN, NCAR, and UKMOn96, distinct upper level *easterly* wind anomaly develops to the east of SST anomaly. Furthermore, the pair of anticyclones, which should develop to the west in the standard Matsuno-Gill pattern, develop to the east of SST anomaly. Due to the combination of eastward shifted anticyclonic response and apparent absence of Kelvin response, the upper level divergence associated with the enhanced precipitation at the SST anomaly consists of meridional divergence and zonal convergence, being to the contrary to the pattern expected from the Matsuno-Gill theory. This seemingly strange response in the tropical latitude can be understood when the unique structure of zonal mean zonal wind in CONTROL (and 3KEQ) of the APE, as will be presented later in section 5.

Except for the loose similarity summerized above, the response in the models differ considerably. Even the amplitude and zonal scale of the mid-

latitude Rossby wave train vary among the models. It is natural to expect that these properties can be related to the structure of the equatorial precipitation anomaly. This poin will be examined later. In some models, appreciable zonal mean response develops especially in higher latitudes. However, as noted, for example, in the ensemble AGCM study on the response to a SST anomaly by Nakajima et al (2004), zonal mean zonal wind in high latitude evolve fairly large amplitude long period (exceeding 100days) variation, so that the zonal mean response presently seen in these experiments of APE may be artifact due to the short of averaging interval, which is specified to be 360 days.

Fig. 2

Fig. 3

3.3 Vertical structure along the equator

Vertical structure of the response, namely anomalies of temperature, zonal wind, and vertical p-velocity, alont the equator in all models are shown in Fig. 4. Diversity of the vertical structure of the response among the models is even larger than that found in the horozontal structure, and the interpretation of the response seems not to be easy as described below.

Altough it seems to be obvious, the feature that can be most easily identifiable as common one to be found in all model, are the general upward motion and mostly positive temperature anomaly above the SST anomaly. In the majority of the models, one can identify three components of signal in

the temperature signal in the troposphere: first, a positive anomaly extending from the surface to about 800hPa possibly resulting from direct effect of the positive SST anomaly below, second a negative anomaly around 600hPa possibly resulting from the parameterized melting of frozen hydrometeor, and, third, a warm anomaly from 300hPa to the tropopause. It might be more surprizing that the temperature anomaly in the lowermost troposphere, which should be directly affected by the SST anomaly, also show quite significant diversity (see Fig. 5 (a) and later discussion). Several factors could contribute to the difference, such as surface flux parameterization, parameterization of turbulence in the mixed layer, parameterization of rain evaporation (or the lack of it), etc. The vertical stutucture of the warm anomaly and vertical velocity alsp vary among the models, presumably resulting from the difference of cumulus parameterization used. The most interesting is GSFC where most of the lower tropsphere is occupied by cold anomaly, which reminds us of the similar cold anomalies found at the location of enhanced precipitation in the composite convectively coupled equatorial waves in APE CONTROL experiment by the GSFC model (Nakajima et al. 2011). In CSIROstd, GSFC, and K1JAPAN, the vertical velocity anomaly in the lower troposphere (p=850hPa) is downward in the convection at the SST anomaly. The development of downward flow at the convetive area may seem to be counter intuitive. but, considering

the existence of strong "basic state" upward motion along the equator, we can safely expect the development of deep convection even with downward perturbation vertical veocity.

The response outside of the SST anomaly also represents complex structure. Namely, the temperature signal to the east of the SST anomaly can not explained as simple Kelvin wave signal, in which case the temperature signal should decay monotonically eastward. There seems to be three components of signal to the east. First is the warm anomaly just below the tropopause, which is very thin (50–100hPa in thickness) and, has Kelvin wave like horizontal structure (not shown here) in many of the model and extends eastward, almost encircling the equator. Second is the warm response largely concentrated in upper troposphere, typically between 400 and 200 hPa pressure surfaces, extending fron the longitude of the SST anomaly to 50 degree to the east. This feature is associated with the upper tropospheric anticyclonoe response in the subtropics (Fig. 2). Third is a warm mid-tropospheric signal placed typically between 300hPa and 850hPa surfaces, longitudinally separated from the heating at the SST anomaly, whose zonal location varies in different models. The most prominent example is the warm anomaly having the zonal extent exceeding 10,000km centered at the longitude of 90° in CGAM (Fig. 4(b)), accompanied by deep downward motion anomaly. It is presumably associated with the equatorward conver-

gent flow in the upper troposphere associated with the return of the Rossby wavetrains to the low latitude, which are originally shed by the convection at the SST anomaly.

To the west of the SST anomaly, temperature anomaly is generally negative. There seems to be two separate components, which are the component in the lower troposphere, lying from 1000hPa to 700hPa, and that in the upper troposphere around 300 hPa. These two seem to depend differently on the models. The negative anomaly in the lower troposhere tends to be prominent in the models with significant negative precipitation to the west of the SST anomaly, i.e., AGUforAPE, CSIROold, DWD, ECMWF05, ECMWF07, GFDL, LASG, and MIT, whereas that in the upper troposphere tends to be prominent in CSIROstd, CSIROold, DWD, GFDL, and UKMO, most of which are characterized with narrow single ITCZ in the CONTROL experiment. The formar model dependence seems not to be unreasonable, but the reason for the latter dependence is unclear. Fig. 4

3.4 Factors controling the intensity of Response

So far, the atmospheric response to the 3KEQ SST anomaly has been qualitatively discussed, with the focus mainly placed on the comparison of spatial structure. In this subsection, we quantitatively examine how the intensity of various aspect of response is related in different models limit-

ting our attention to small number of quantities which, we hope, sketch gross feature of the response. As descibed below, we can identify several positive correlation that could be expected from the dynamical or budget constraints, but, at the same time, existence of large cattering among differnt models should be taken to be important result of intercomparison.

Fig. 5(a) shows the relationship between the amplitude of precipitation response and the amplitude of temperature response at 925hPa averaged within $\pm 5^\circ$ latitude band. (In the following, amplitude is defined as the difference between the maximum value and the minimum value unless otherwise noted.) First thing to note is that the precipitation amplitude and the low level temperature amplitude are linearly well correlated, with only two exception of K1JAPAN and AGUforAPE. The rather clean relationship is a bit surprising considering the wide variety of the implimentations of physical process in the models. At the same time, however, the large scattering in each variables does imply existence of large ambiguity among the models. Fig. 5(b) shows the relationship between the amplitude of mixing ratio response at 925 hPa, multiplied by L/c_p to be represented in terms of its contribution to latent heating, and the amplitude of precipitation. Although general positive correlation can be noticed in the scatter plot, the correlation is looser than that in Fig. 5(a). The relatibve disperity of mixing ratio amplitude is even larter than that of temperature amplitude. Fig. 5(c)

shows the relationship between the amplitude of precipitation response and the amplitude of zonal wind response at 925hPa. Between the two, we can again note positive correlation, which is expected based on both dynamics and water vapor budget. Further again, the scatter is large among the models; the existence of considerable scattering is quite understandable if we recall the variety of the structure of dynamical response described in the previous subsection.

Fig. 5(d) and (e) show the relationship between the amplitude of precipitation response in 3KEQ experiments and the zonally averaged precipitation in corresponding CONTROL experiments averaged within $\pm 5^\circ$ and $\pm 15^\circ$ latitude bands, respectively. Positive correlation found in these figures seem to be reasonable because, as is pointed out earlier in this section, the latitudinal structure of precipitation anomaly reflects general feature of precipitation in CONTROL experiments in the corresponding models. Scattering among the models is smaller for the average of $\pm 15^\circ$ latitude bands, where meridional structure of ITCZ is eliminated. Still, the ratio between the average precipitations of MIT and K1JAPAN reaches as large as 3.

Fig. 5(f) and (g) show the relationship between the amplitude of precipitation response and the amplitude of surface latent heat flux averaged within $\pm 5^\circ$ and $\pm 15^\circ$ latitude bands, respectively. For $\pm 5^\circ$, these two vari-

ables are not correlated well. For $\pm 15^{\circ}$, certain degree of correlation can be identified, but it may be heavily affected by rather isolated point of MIT, without which other data points are merely clustered around the average.

Finally, we examine the relationship between the intensities of tropical precipitation anomaly and the extratropical wave amplitude. Fig. 5(h) and (i) show the relationship between the amplitude of precipitation response and the amplitude of geopotential height anomaly on 250hPa and 925hPa, respectively. Here, the amplitude of geopotential height anomaly is calculated as the difference between the maximum and minimum values of the eddy component geopotential height, i.e., departure from the zonal mean values. Except for the difference of absolute value of wave amplitude at the two levels, we can note similar tendency in Fig. 5(h) and (i), suggesting common equivalent barotropic structure of the extratropical response. We can also identify loose positive correlation, but the considerable scattering of wave amplitude can not be overlooked as a trivial issue. Fig. 5

3.5 Linearity of response to localized SST anomaly

By comparing result of 3KEQ and 1KEQ experiments, we can obtain some idea on how much linear the response to equatorial local SST anomaly is. Because it is quite cumbersome to present all the details of the response of 1KEQ and the purpose is to compare the results of 1KEQ and 3KEQ

quantitatively, we do not show the structure of response.

Fig. 6(a) shows the scatter plot of precipitation anomaly averaged over the area of SST anomaly for 1KEQ and 3KEQ. If the response is linear, the data points should distribute along the line with the slope of 3. Actually, the points scattered show some mount of nonlinearity; the departure from the linear relationship is more significant for the models with more intense precipitation anomaly, suggesting the existence of positive feedback loop via moisture convergence etc. Fig. 6(b) shows the scatter plot of the amplitude of precipitation anomaly averaged in $\pm 15^{\circ}$ latitude band. Here reverse kind of nonlinearity can be noted; the ratio between the response of 1KEQ and 3KEQ is almost precicely 3 in the models with weak anomaly (e.g., K1JAPAN), while it is significantly smaller than 3 in the models with intense anomaly (e.g., MIT).

Fig. 6(c) shows the scatter plot of the amplitude of extratropical geopotential anomaly at 250hPa in 1KEQ and 3KEQ. Although The amplitude in 3KEQ and 1KEQ is certainly positively correlated, the ratio between the amplitude in 3KEQ and that in 1KEQ far less than 3, which may indicate the presence of some nonlinearity that suppress that results in saturation of extratropical wave amplitide. However, we should be cautious about the possible contamination by the background wave activity. In fact, the quasi stationary wave amplitide in CONTROL experiment is as large as 40–70m,

depending on the model. If we could extract the excess amplitudes over the above "background" value in 3KEQ and 1KEQ experiments, the constant of proportionality of the amplitude in 3KEQ to that in 1KEQ would be larger. Quantitative examination of this point requires more careful statistical considerations and is left for future research. Fig. 6

4. Response to wavenumber one variation of SST along the equator

In this section, the response to the wavenumber one variation of the equatorial SST of 3KW1 cases are described briefly.

4.1 Precipitation response

In Fig. 7 we compare time mean precipitation anomaly emerging in the 15 AGCM runs of APE. A common character of the precipitation response is the dominance of zonal wavenumber one structure in wide range of latitudes. In most of the models the signature of the anomaly at the maxima along the equator is definitely positive. The only exception is CSIROstd, in which negative anomaly prevails along the equator, so that only small positive anomaly is found. Even in this model, however, the anomaly averaged in the latitudinal band of $\pm 15^{\circ}$, the signature of the anomaly is definitely

positive.

As will be shown shortly later, the phase of the equatorial precipitation anomaly is shifted by about 30 degrees west of the SST anomaly. The amplitude of the anomaly at the equator is comparable to the zonal mean precipitation in the CONTROL experiments by the corresponding models, so that the actual amount of precipitation in the suppressed region 3KW1 is virtually zero in most of the models. In spite of the quite strong modulation forced by the SST anomaly, latitudinal structure of ITCZ precipitation in unperturbed, CONTROL experiment in the corresponding models are preserved to certain extent. For example, double ITCZ structure is clearly seen in the anomaly of NCAR. THe latitudinal width of the ITCZ at the longitudes of enhanced precipitation in each models is similar to that in the CONTROL.

Wavenumber one modulation of precipitation is alsp notable in the midlatitude baroclinic zones. The phase of the precipitation anomaly is shipted about 90 degrees to the east of the SST anomaly. The models can be classified in two categories, models that exhibit significant subtropical precipitation anomaly, which are ECMWF07, GSFC, MRI, and NCAR, and the ones that do not. In the former type of the models, the subtropical precipitation anomaly develops to connect the equatorial and midlatitude precipitation anomaly, implying the presence of wave propagation from deep

tropics. Fig. 7

4.2 Horizontal structure of Response

Horizontal structure of the response, namely anomalies of horizontal wind and geopotential height, on the 250hPa and 850hPa surface are shown in figure 8 and 9, respectively. The horizontal structure of the dynamical response is rather similar among the models, and again, is dominated by zonal wavenumber one structure. The phase of pressure perturbation is almost constant within tropics, so that whole of the tropics is mostly covered with a single wavenumber one baroclinic disturbance. Also noted in most of the model is the presence of significant zonal mean westerly acceleration in the upper troposphere. The response in the extratropics is generally barotropic. The phase relation between the tropical and extratropical pressure anomaly at the edge of troposphere is in-phase in the lower troposphere and out-of-phase in the upper troposphere.

In the tropics of upper troposphere, a high pressure center is located to the east of the phase of highest SST anomaly by about 20 degrees, or 50 degrees to the east of the rainfall maximum. Corresponding to the phase relationship between the rainfall and pressure anomaly, the upper level outflow from the enhanced precipitation anomaly diverges almost poleward, with little zonal wind component, in most models. The westerly anomaly

is distributed mostly outside of the positive rainfall anomaly, and the low pressire anomaly in the longitudes of suppressed precipitation is devided at the equator. In the lower troposphere, there is equatorward flow to the positive rainfall anomaly. Superposed to this convergent flow, in most models, there is significant westerly anomaly, which is consistent with the pressure response that is negative to the easteast of the precipitation anomaly.

Both in the upper and lower troposphere, in some models, trace of Rossby wave propagation from the tropics can be noted, whose evidence is westward phase tilt from lower to higher latitudes. This phase shift should presumably associated with equatorward transport of westerly momentum, which should contribute to the westerly acceleration in the tropics noted rarlier.

Fig. 8

Fig. 9

4.3 Vertical structure along the equator

Vertical structure of the response, namely anomalies of temperature, zonal wind, and vertical p-velocity, alont the equator in all models are shown in figure 10. Compared with the very widespread variation in 3KEQ (Fig. 4), the diversity among the 3KW1 experiments is to a lesser degree. The vertical structure of the response is, however, not so simple.

As in 3KEQ, four components seem to be exists in the vertical structure of temperature signal, i.e., a very shallow structure just below the

tropopause, an upper troposheric signal with 200 hPa thickness, mid tropospheric signal located considerably to the east of the SST anomaly, and the lowermost tropospheric signal directly forced by the SST anomaly. Again as in 3KEQ, the amplitude, altitude, etc. varies among the models. It should be noted is that, even at the lowermost troposphere, the longitude of maximum temperature perturbation is not located at the maximum of the SST anomaly but is shifted to the east.

Longitudinal variation of vertical velocity anomaly generally follows the variation of precipitation along the equator in each model. However, as in 3KEQ experiments, its vertical structure is strongly model dependent; part of the variability presumably results from the difference of physical parameterizations used, but the response of CSIROstd, dominated by downward motion anomaly in lower troposphere everywhere at the equator, is due to the mostly negaitve precipitation anomaly in the model.

An notable feature commonly realized in all of the models is the phase of the vertical velocity anomaly and that of the temperature anomaly differ significantly. The differnce of the phases is not small in the upper troposphere, they are in almost quadrature in the middle troposphere. Fig. 10

4.4 Quantitative comparison of wavenumber one component

Because the response in the 3KW1 experiments is dominated by the zonal wavenumber one structure as has been touched above, we try to compare the compare the response in various models quantitatively, extracting the wavenumber one components of several variables of the response structure.

Fig. 11(a) compares the amplitude and phase of the precipitation anomaly averaged in the latitudinal band of $\pm 15^\circ$. Altough the amplitude scatter over a relative factor of about 2, the scattering of phase is well concentrated within 30 degrees. The scattering of the surface latent flux anomaly, shown in Fig. 11(b), are even smaller. On the othre hand, the amplitude and phase of the anomaly of low level mixing ratio, shown in Fig. 11(c), diverges a lot; the amplitude ranges over a relative factor of about 4, and the phase varies over almost 90 degrees. We should notify that, because the mean surface pressure in GFDL is 1000hPa instead of 101325Pa specified in other models, the large amplitude in GFDL should be regarded as abbreration. Even excluding it, however, the amplitude vary exceeding relative factor of 2.

Fig. 11(d)–(f) compare the amplitude and phase of geopotential anomaly at 20, 40, and 60 degrees latitudes. The amplitude and phase at 20 degrees latitude are distributed in a fairly compact region; the variance looks even smaller than that of the precipitation (Fig. 11(a)). At 40 degrees latitude,

the variance of phase increases slightly, but the amplitude variance is still small. However, at 60 degrees latitude, the scattering increases to a quite large degree; the phase variation reaches almost 90 degrees, and the amplitude variance exceeds the relative factor of 5, showing a large degree of difference in the propagation of the wavenumber one anomaly into high latitudes among the models. Fig. 11

4.5 Factors controling the intensity of Response

As the final element of intercomparison, as done for 3KEQ, we quantitatively examine how the intensity of various aspect of response is related in different models. (As for 3KEQ, the amplitudes of variables in the following description are defined as the difference between the maximum value and the minimum value unless otherwise noted.)

Fig. 12(a) shows the scatterplot of the amplitude of precipitation anomaly and the zonal mean precipitation in the CONTROL experiment, both of which are averaged within $\pm 5^\circ$ latitudes. Good correlation is found between the two quantities; the colleration seems to be better than for 3KEQ (Fig. 5(d)). ECMWF05 exhibits exceedingly large precipitation response even scaled by the unperturbed precipitation of CONTROL experiment.

Fig. 12(b) shows the scatterplot of the amplitude of precipitation anomaly and that of the meridional convergence at 925hPa calculated from the merid-

ional wind component at ±5° latitudes. Again, good correlation is found between the two quantities. In contrast, such a good correlation does not exists between the precipitation amplitude and the zonal convergence (not shown), implying that the precipitation anomaly in 3KW1 is supported mainly by meridional convergence.

Fig. 12(c) shows the scatterplot of the amplitude of precipitation anomaly and that of the meridional convergence at 925hPa calculated from the meridional wind component at ±15° latitudes. Compared with similar scatter plot for ±5° latitudes presented just before, the correlation between the two data seems to be worse, suggesting the existence of other contributing factors. In addition, it is noted that the relative degree of scattering of the two variables is reduced. ECMWF05 is not "outlier" in this scatter plot.

Fig. 12(d) shows the scatterplot of the amplitude of precipitation anomaly and that of surface latent heat flux averaged within ±15° latitudes. The correlattion between the two is quite remarkable, and, moreover, the absolute value of the latter is larger than half of the former, implying the dominating role of latent heat flux variation in the variation of tropical precipitation.

Fig. 12(e) shows the scatterplot of the amplitude of precipitation anomaly and the zonal mean precipitation in the CONTROL experiment, both of which are averaged within ±15° latitudes. In contrast to the similar plot for ±5° latitudes (Fig. 12(a)), the correlation between the two quantities is

much reduced, being even worse than that in 3KEQ experiments (Fig. 5(e)).

Finally, Fig. 12(f) shows the scatterplot of the amplitude of precipitation and the zonal mean zonal wind acceleration at 200hPa averaged within $\pm 5^\circ$ latitudes. We can only find the exisetence of large scatterings; no significant correlation can be noted. The situation is simiar for similar scatter plot for the $\pm 15^\circ$ latitudes band. This lack of correlation implies the existence of other factors in the process of zonal wind acceleration. This may be unsurprizing if we recall the considerable variation seen in the latitudinal structure of rainfall anomaly (Fig. 7). Fig. 12

5. Excitation Mechanism of Response

We have explored, although to a limited extent, the response of the atmosphere of an aqua planet to the two kinds of variations of SST placed on the equator, 3KEQ and 3KW1, exemplified in a number of AGCM runs participating the APE. The results show that, without doubt, the response of the AGCMs is strongly model dependent in spite of the unified and simple setup. This finding is an important first step to the attainment of one of the purpose of this series of the APE, i.e., to determine the variation of the ciruculation response to a localized or planetary scale anomaly in tropical SST. However, the other purpose, i.e., the identification of processes that determine the sstructure of response, is virtually untouched.

In this section, we try to identify some of the important dynamical agents that shape the structure of the response. Namely, we try to understand the reason why the dynamical response to an localized equatorial SST anomaly differ so much from the classical Matsuno-Gill pattern. For this purpose, we present another pair of aqua planet experiments that also examine the response to an localized equatorial SST anomaly but with different "basic state" meridional SST distribution. The response exemplified in this pair will be compared with the response to 3KEQ SST anomaly in one of the models descibed previously, both of which are analyzed indentifying the Rossby wave source terms as was done by Sardeshmukh and Hoskins (1988). Additionaly, we examine the response to 3KW1 SST anomaly in one of the models, but we do not go into detail because full more thorough analysis seems to be required to understand the important features of the response in 3KW1 case, e.g., variable degree of equatorial super rotation, longitudinal modulation of mid-latitude storm tracks, etc.

5.1 Mechanism of Response to localized equatorial SST anomaly

The pair of experiments we present here in order to contrast the response in it with that of 3KEQ described earlier are the pair of runs conducted using a modified version of AGUforAPE model in which Arakawa Schubert scheme (Pan and Randall 1998) is employed for cumulus parameterization

instead of Emanuel scheme (Emanuel and Zivkovic-Rothman 1999) with FLAT and FLAT3KEQ SST distribution defined in section 2. Our motivation of employing this particular specification is as follows: we use the FLAT and FLAT3KEQ SST for comparison as they are one of, or a simple modification of, the SST specifications for the APE, so that other researchers can easily verify our supplimentary experiment, one of which, FLAT experiment, is already conducted by each participating models. Our motivation of not employing the original version but employing the modified version of AGUforAPE model is that the response emerging in the modified model is similar to the response obtained by Hosaka et al (1998) including the enhancement of precipitation to the east of the SST anomaly, which does not appear in most of the 3KEQ experiments (Fig. 1). Because our attempts here is not to extract the difference between the response in the different pair but to understand the mechanism of the response exemplified in each pair, the different choice of cumulus parameterization makes nothing inconvenient.

Fig. 13(a)–(d) show the response of the atmosphere to the 3KEQ SST anomaly with the FLAT SST is used as the "unperturbed" SST profile instead of CONTROL. As decribed below, the response can be explained much more easily reffereing the classical equatorial thermal response theory of Matsuno (1966) and Gill (1980). As in the response in the standard

3KEQ experiments (Fig. 1), a distinct positive anomaly of precipitation develops above the SST anomaly (Fig. 13(a)). The meridional extent of the precipitation anomaly is larger than that in the standard 3KEQ experiments, and there is a pair of zones of negative precipitation anomaly along the latitudes $\pm 10 \sim 15^\circ$ where the precipitation maxima of ITCZ is located in FLAT experiment (see Fig. 15(a)). It is notable the precipitation between the double ITCZs increases to the east and decreases to the west of the SST anomaly. This is the character of precipitation resonse that appear in Hosaka et al (1998). The response of dynamic field in the upper (Fig. 13(b)) and lower (Fig. 13(c)) troposphere includes a number of features expected from the classical Matsuno-Gill pattern: the eastward extending equatorially confined baroclinic Kelvin wave like feature, a pair of baroclinic Rossby response located around $\pm 5 \sim 20^\circ$ latitudes located definitely to the west of the SST anomaly in longitude. A pair of extratropical Rossby wavetrains is noted as in the standard 3KEQ cases, but they propagates to higher latitudes, so that they do not interact with the tropical response near the SST anomaly. The vertical structure along the equator (Fig. 13(d)) also has the feature directly expected from the classical pattern: positive temperature anomaly develop to the east from the enhanced convection above the SST anomaly, except for minor modification resulting from parameterized melting of icy hydrometeor. Zonal flows converges

from both directions in the lower troposphere and, although obscured by the general westerly acceleration, diverges in the upper troposphere. Fig. 13

Now that we have the contrasting pair of response to localized equatorial SST anomaly, we examine how the response develops in each case, by which, we hope, the unique character of the response in 3KEQ experiments of APE would be clearly notified. In spite that one of the important feature of 3KEQ response appears to be the absence of the equatorial Kelvin response, the principal origin of the uniqueness resides in generation and behavior of Rossby response, as demonstrated in the analysis below. The analysis is done only for uppper troposphere, where Rossy waves are mainly generated.

In order to describe the dynamical structure of the response clearly, we separate the horizontal wind response into rotational and divergent components. As demonstrated in the diagnosis of Rossby wave source by Sardeshmukh and Hoskins (1988), the former represents the structure of Rossby waves generated by the source term associated with the latter. The definition and calculation method of the rotational and divergent components and the Rossby wave sources are presented in section 2.

Fig. 14 (a) and (b) show the rotational component of horizontal wind response in 3KEQ response and FLAT3KEQ response, respectively, whereas fig. 14 (c) and (d) show the divergent components. The contribution of zonal mean zonal wind response is removed to show the behavior of Rossby waves

more clearly.

A striking difference between the Rossby wave structure in the two cases is the signature of the Rossby response over the SST anomaly. For FLAT3KEQ, the anticyclonic Rossby response develops to the west of the SST anomaly. As a result, although there is a slight eastward shift, strong equatorward flow exists near the SST anomaly, which is a character noted in the structure of equatorial thermal response by Gill(1980). To the contrary, for 3KEQ, anticyclonic Rossby response is seen to develop to the *east* of the SST anomaly. It is associated with *poleward* rotational flow near the SST anomaly and zonal flow *toward* the positive anomaly to the east, which, combined with the associated positive poleward pressure gradient, would cancel possible Kelvin response. Such cancellation is working with extreme degree in other model, e.g., CSIROold, ECMWF07, GFDL, and UKMO (Fig. 2(c),(g),(h),and,(o)), where strong easterly response can be noted to the east of the SST anomaly. The *cyclonic* Rossby response to the west is also reverse in signature with the ordinary expected anticyclonic response.

The distinct difference in the structure of Rossby response in the 3KEQ and FLAT3KEQ cases can be understood if we examine the meridional structure of upper tropospheric absolute vorticity, and the distribution of Rossby wave sources in both cases. In fig. 15(a)–(d), the meridional structure of the tropical region in "unperturbed" experiments, CONTROL and

FLAT, are shown. In FLAT experiment, the tropical precipitation (solid line in Fig. 15(a)) has the double ITCZ structure, which is associated with the upward flow broadly distrobuted in low latitude (not shown here), resulting in rather small meridional gradient of zonal mean zonal wind (solid line in Fig. 15(b)). Correspondingly, absolute vorticity in low latitude varies almost smoothly from the equator to mid-latitudes (solid line in Fig. 15(c)), so that the region of zero-absolute vorticity exists only close to the equator, and the equivalent beta factor (solid line in Fig. 15(d)) has non-zero value all over the tropics. On the other hand, in CONTROL experiment, the tropical precipitation (broken line in Fig. 15(a)) is concentrated at the equator, which is associated with the upward flow narrowly confined near the equator (not shown here), because of near conservation of angular momentum in the upper level outflow of the Hadley circulation, resulting in a fairly wide region of zero-absolute vorticity in the tropics (broken line in Fig. 15(c)). Correspondingly, the equivalent beta factor (broken line in Fig. 15(d)) is very small in the tropics, but it increases sharply approaching the mid-latitude jet. It should also noted that, due to the difference of angular momentum of the upper tropospheric air in CONTROL and FLAT, reflecting the difference of the latitude of the origin of the air parcel leaving the planetary surface, the zonal mean zonal wind velocity differ considerably between the two cases; westerly wind is much stronger in CONTROL

and is extending to much lower latitudes (Fig. 15(b)).

The difference of the upper tropospheric distribution of absolute vorticity and the effective beta factor, combined with the structure of divergent conponent of flow response, results in distinct difference of Rossby wave source between the two cases. Fig. 14 (f), (h), and (j) show the distribution of the advective, divergent, and total Rossby wave souece in the FLAT3KEQ response, respectively. Because both appreciable the effective beta factor and non-zero absolute vorticity exist over the wide area except at the very narrow region near the equator, both advective and divergent source develops in wide area near the SST anomaly, the development of divergence in off equatorial latitude (Fig. 14(d)) assures the existence of the divergent source. The two component being combined, the total source is distributed in wide area of tropics. As a result, significant westward propagating equatorial Rossby wave is generated, manly due to the digergent source, as expected in the Matsuno-Gill pattern. Rossby wave is also generated with significant amplitude near mid-latitude jets, The Rossby wave propagates to higher latitudes and then return to lower latitude, which, however, can not invade the tropical region due to the presence of a broad zone of zonal mean easterly (solid line in Fig. 15(b)); so that the Rossby response does not interfare the development of Kelvin wave component. Whole of the result is, after all, the development of the "standard" Matsuno-Gill pattern. The

Kelvin response to the east is associated with meridional convergence near the surface (not shown here), resulting in the enhancement of precipitation along the equator (Fig. 13(a)), being similar to the structure of precipitation response pattern in Hosaka et al (1998).

Fig. 14 (c), (g), and (i) show the distribution of the advective, divergent, and total Rossby wave souece in the 3KEQ response, respectively. Because appreciable the effective beta factor exists only far from the equator (Fig. 15(d)), the advective source is significant only near the mid-latitude jets, and it is anti-cyclonic. The divergent source is also weak in deep tropics, where absolute vorticity is nearly zero (Fig. 15(c)). The two component being combined, the total source is also small near the equator. As a result, westward propagating equatorial Rossby wave is not generated, which is the character different from the Matsuno-Gill pattern. Instead, Rossby wave is generated with significant amplitude near mid-latitude jets, where, because the zonal mean zonal wind is already strong westerly, Rossby wave generated here can not propagate westward, but, instead, develop as the stationary barotropic wavetrain propagating eastward (Fig. 2 and Fig. 3). As noted earlier, bacause of the strong westerly jet, the Rossby wavetrains do not reach high latitudes but soon curved back to the low latitudes. Furthermore, the Rossby wavetrains are allowed to invades deep tropics because the zonal mean westerly flow extends to very low latitudes (broken line in

Fig. 15(b)). This is the true character of the Rossby signal to the east of the SST anomaly in 3KEQ response. There are also region of cyclonic sources at around $\pm 40^{\circ}$ latitudes, but they can not exite Rossby waves with large amplitude because of the large mis-match between the fast westerly flow velocity and small intrinsic westward phase velocity of Rossby wave at that latitudes resulting from the reduction of the effective beta factor (broken line in Fig. 15(d)) due to the curvature of the meridional profile of westerly jet.

It should be noted that although the structure of the response of 3KEQ, which is characterized with the *eastward* development of Rossby waves, appears to be similar to that discussed by Lim and Chang (1983), the mechanism is significantly different. That is, while Lim and Chang (1983) pointed out the important role of basic wind shaping the structure of the response of tropical atmosphere to thermal forcing, they remained to consider the Rossby wave source only to be the divergent source in the present definition. In 3KEQ response, not the divergent source but the advective source is primarily important.

A significant reduction of precipitation immediately to the west of the SST anomaly as the response to 3KEQ SST anomaly in the most of the models (Fig. 7) requires explanation. Similar negative precipitation anomaly appeared in Hosaka et al (1998), and was interpreted as a result of Rossby

response to the west of SST anomaly by Nakajima et al (2004). The explanation is effective for Hosaka et al (1998) and Nakajima et al (2004), where Rossby response to the west did appear. However, it does not apply to 3KEQ cases in the APE, where Rossby response to the west did not appear. One possible factor creating the negative precipitation anomaly is the near surface westerly wind response that is located at the edge of, and is driven by the SST anomaly (Lindzen and Nigam, 1987). This component of wind is basically confined to the surface mixed layer, but a trace of it can be seen even at 850hPa (Fig. 3). The examination of this point is, however, not an easy task because, as noted before, even the relationship between the SST and the mean temperature of mixed layer is strongly model dependent (Fig. 5(a)). We do not go into this issue in the present paper.

Lastly, we note on the behavior Kelvin response in 3KEQ. If we seek carefully, bearing the strong interfarence from the Rossby waves in mind, we can "rediscover" the trace of Kelvin response other than the thin positive temperature anomaly mentioned earlier: in many of the models, we can note the presence of westerly zonal wind anomaly and easterly zonal wind anomaly confined within $\pm 10^\circ$ latitudes along the equator emerging from 100 degrees to the east the SST anomaly and encircling the equator more or less overlapped by the perturbation by the Rossby response invading the tropics (Fig. 2 and Fig. 3). In other words, the Kelvin response can be

identified as the zonal wavenumber zero component.

In the above consideration, the mechanism of the response is sketched only in a horizontal plane; the response in the AGCM has three-dimensional structure, so that the understanding of its intricate feature may well require additional consideration with three-dimensional dynamics taken into account. Those issues are left for future research.

Fig. 14

Fig. 15

5.2 Mechanism of Response to large scale variation of equatorial SST anomaly

Finally, mechanism of response in 3KW1 is exanimed briefly. From the 15 AGCM runs with 3KW1, we choose two runs, DWD and NCAR, and diagnose the Rossby wave source. The reason for this choice of experiments is that these two are the end-menbers of the set of the experiments in following two aspects. First, with CONTROL SST, DWD is characterized with a narrow single ITCZ at the equator whereas NCAR exhibits distinct double ITCZ. Second, with 3KW1, DWD exhibits smallest zonal wind acceleration at the equator whereas NCAR exhibits the largest (Fig. 12(f)). With this choice, we hope that we could survey common and varying features in the response development, which may be useful in more through examination of 3KW1 cases in the APE in a future study.

Fig. 16 (a)–(j) display the dynamical structure and Rossby wave source

in the upper troposphere response to the zonally wavenumber one varitation of SST near the equator represented in the 3KW1 experiments of DWD and NCAR. Comparing the rotational component of wind response (Fig. 16 (a) and (b)), it is noted that the response is stronger in NCAR, whose response has singinficant phase tilt in latitude; the phase tilt suggests negative correlation between the zonal and meridional disturbance wind components, i.e., equatorward transport of zonal momemtum. Such phase tilt is absent in DWD. This difference is not inconsistent with the difference of zonal wind acceleration realized between the two models (Fig. 12(f)).

The response of divergence (Fig. 16 (c) and (d)) differ significantly in low latitudes; the response in DWD shows rather simple wave like variation confined the equator, whereas considerable off-equatorial component exist in NCAR. Namely, a pair of divergence exists centered at $(\lambda, \varphi) = (-90°, \pm 15°)$, which is driven by the off-equatorial positive precipitation anomaly (Fig. 7 (n)). The most notable difference is the presence in NCAR or absence in DWD of the pair of anti-cyclonic sources around $(\lambda, \varphi) = (-90°, \pm 15°)$, which is related to the divergence anomaly in NCAR (Fig. 16 (c) and (d)). Closely examined, the wave source is distributed with some degree of meridional tilt in NCAR; it is located more westward in higher latitudes. The tilted distribution of the wave source, is, again, not inconsitent with the development of tilted Rossby wave response (Fig. 16 (b)).

The general weak intensity of higher latitude response (Fig. 16 (a) and (b)) in spite of the appreciable existence of wave sources (Fig. 16 (i) and (j)) presumably result from the mismatch of the wind speed of westerly jet and westward instrinsic phase velocity of the Rossby wave in extratropics.

Nevertheless, we can identify certain similarity between the response in two models. In both models, the divergent component of wind response is dominated by meridional flow. This is because of the zonally elongated shape of the precipitation, or divergence, anomaly. Comparing the Rossby wave sources (Fig. 16 (e,g,i) for DWD, and (f,h,j) for NCAR), it is identified, as a common feature, that the Rossby response (Fig. 16 (a) and (b)) develops to the east of the sources (Fig. 16 (i) and (j)). This results from the strong westerly jets around these latitudes. These feature can be noted in most of the models, and the mechanism is common to that working in a simple numerical experiment concerning the response of mid latitude atmosphere to tropical SST variation by Inatsu et al (2002). Fig. 16

6. Concluding remarks

The variety of precipitation and circulation structures that appear in the numerical experiments conducted in the Aqua Planet Experiment Project in response to equatorial SST anomaly are compared. A short summary of the comparison is presented in the abstract and not repeated here.

In addution to the comparison of the results of the experiments in APE, we have shown the result of a supplemental pair of experiments showing the response of aqua planet GCM to a localized equatorial SST anomaly over the FLAT SST profile. The comparison between the response in this supplemental experiments and the response employing the CONTROL SST profile demonstrates quite large degree of sensitivity of the response to the profile of "basic state" SST. This strong sensitivity strongly suggests that both the dynamics of the response to SST anomaly in general and its variety of representation in different models also dependend on the choice of basic state profile of SST. It would be useful, as a small extention of the APE, to conduct model intercomparison on the response to equatorial SST anomaly with the basic state SST profiles other than the CONTROL; it will provide additional useful information on the participating models. The applicability to real atmosphere would be more strengthened. We already conducted a small subset of such experiment with AGUforAPE model with several choice of cumulus parameterizations and spatial resolutions, one of which is the case presented in this paper. The result suggests, as is expected, that the structure of the response does depends strongly on cumulus parameterization employed and the resolution. The details will be described elsewhere.

We conducted a preliminary survey on the mechanism of the remote

dynamical response, i.e., that of wind and pressure field, but we have not examined the remote response of precipitation in any detail. The remote response of precipitation is expected to be more difficult to understand because it shall be doubly complicated by cumulus parameterization: the development of direct, or near field, precipitation response above the SST anomaly is, as described in this paper, strongly model dependent, so that the remote dynamical response is model dependent, and, the remote precipitation response results from already model dependent dynamical response, through a manner which is model dependent. The situation is further complicated by possible dependence on the structure of basic state precipitation distribution with the "unperturbed" SST, which is, in itself, model dependent. Solution of this complicated issue will possibly require the next series of APE with more systematic experimental design. One direction that could be useful is to examine the sequence of response development in an ensemble experiment (e.g. Jin and Hoskins, 1995; Nakajima et al,2004). More detailed analysis of wave propagation would also be useful using the wave activity diagnosis of Takaya and Nakamura (2001). Analysis on the transient disturbances would be also necessary.

In this paper, we did not examine the properties of transient disturbance, namely the analysis of composite structure of convectively coupled equatorial waves as done by Nakajima et al (2011) for the experiments with

CONTROL SST profile is not performed. The analysis of these points is worth doing, particularly because behavior of such disturbances may be important in shaping the stationary response structure. Although the space time spectra of precipitation and OLR are presented in the APE-ATLAS (Williamson et al. 2011), unfortunately, full set of time series of three dimensional data was not collected in the APE data archive. The limited data, for example the upper tropospheric wind field, suggest possibly significant response of various character of transient disturbances, in depth examination of them, which requires more complete dataset, is left for future series of APE.

Finally, it should be noted that we did not examine the detailed structure and dynamics of the rainfall anomaly that develop as the direct response to the SST anomaly. Preliminary survey of time series of precipitation shows that, as is in the previous study (Hosaka et al. 1998), the precipitation anomaly results not from smoothly distributed increase of rainfall but from the increase of density or frequency of various kind of precipitating disturbance. This point would be an interesting issue, but, due to the rather coarse resolution of the participating models in the APE project, the physical reality of the exemplified behavior may be questionable. Model with higher resolution (e.g., Yoshioka and Kurihara, 2008) would be necessary. Considering the diversity of the gross response of precipitation and other

variables (e.g., Fig 5 and 6), understanding of the issue of direct response requires rather complete set of the parameterization tendency, not only that of cumulus parameterization but also those of boundary layer processes etc. Even with mostly complete datasets, complexity resulting from various feedback and interaction among the possibly contributiong processes might make the understanding of the issue a difficult task. This is also left for future research.

Acknowledgements

Numerical integration of AGU model were performed at the Earth Simulator Center. Analysis software and local computational environments were constructed by the use of the resources of GFD-DENNOU-CLUB (http://www.gfd-dennou.org), including GPhys (http://ruby.gfd-dennou.org), spmodel (http://www.gfd-dennou.org/library/spmodel), and DCL (http://www.gfd-dennou.org/library/dcl). This work was supported by Grants-in-Aid(B) for Scientific Research (12440123 and 21340139).

References

Bjerknes, J., 1969: Atmospheric teleconnections from the equatorial pacific 1. *Monthly Weather Review*, **97(3)**, 163–172.

Blackburn, M., and B. Hoskions, 2011: Context and aims of the aqua planet experiment. *J. Meteor. Soc. Japan*, **??**, submitted.

Emanuel, K., and M. Zivkovic-Rothman, 1999: Development and evaluation of a convection scheme for use in climate models. *Journal of the atmospheric sciences*, **56(11)**, 1766–1782.

Gill, A., 1980: Some simple solutions for heat-induced tropical circulation. *Quarterly Journal of the Royal Meteorological Society*, **106(449)**, 447–462.

Held, I., and A. Hou, 1980: Nonlinear axially symmetric circulation in a nearly invicid atmosphere. *Journal of the Atmospheric Sciences*, **37**, 515–533.

Hoerling, M., and A. Kumar, 2002: Atmospheric response patterns associated with tropical forcing. *Journal of climate*, **15(16)**, 2184–2203.

Hosaka, M., M. Ishiwatari, S. Takehiro, K. Nakajima, and Y. Hayashi, 1998: Tropical precipitation patterns in response to a local warm sst area placed at the equator of an aqua planet. *JOURNAL-METEOROLOGICAL SOCIETY OF JAPAN SERIES 2*, **76**, 289–305.

Hoskins, B., and D. Karoly, 1981: The steady linear response of a spher-

ical atmosphere to thermal and orographic forcing. *Journal of the Atmospheric Sciences*, **38(6)**, 1179–1196.

Inatsu, M., H. Mukougawa, and S. Xie, 2002: Stationary eddy response to surface boundary forcing: Idealized gcm experiments. *Journal of the atmospheric sciences*, **59(11)**, 1898–1915.

Jin, F., and B. Hoskins, 1995: The direct response to tropical heating in a baroclinic atmosphere. *Journal of the atmospheric sciences*, **52(3)**, 307–319.

Lim, H., and C.-P. Chang, 1983: Dynamics of teleconnections and Walker circulations forced by equatorial heating. *Journal of the atmospheric sciences*, **40(8)**, 1897–1915.

LINDZEN, R., and S. Nigam, 1987: On the role of sea surface temperature gradients in forcing low-level winds and convergence in the tropics. *Journal of the Atmospheric Sciences*, **44(17)**, 2418–2436.

Matsuno, T., 1966: Quasi-geostrophic motions in the equatorial area. *J. Meteor. Soc. Japan*, **44(1)**, 25–42.

NAKAJIMA, K., E. TOYODA, M. ISHIWATARI, S. TAKEHIRO, and Y. HAYASHI, 2004: Initial development of tropical precipitation pat-

terns in response to a local warm sst area: An aqua-planet ensemble study. *J. Meteor. Soc. Japan*, **82(6)**, 1483–1504.

Nakajima, K., Y. Yamada, Y. Takahashi, M. Ishiwatari, W. Ohfuchi, and Y.-Y. Hayashi, 2011: The variety of spontaneously generated tropical precipitation patterns found in ape results. *J. Meteor. Soc. Japan*, **??**, submitted.

Neale, R., and B. Hoskins, 2000a: A standard test for agcms including their physical parametrizations: I: The proposal. *Atmospheric Science Letters*, **1(2)**, 101–107.

Neale, R., and B. Hoskins, 2000b: A standard test for agcms including their physical parametrizations. ii: Results for the met office model. *Atmospheric Science Letters*, **1(2)**, 108–114.

Pan, D., and D. Randall, 1998: A cumulus parameterization with a prognostic closure. *Quarterly Journal of the Royal Meteorological Society*, **124(547)**, 949–981.

Sardeshmukh, P., and B. Hoskins, 1988: The generation of global rotational flow by steady idealized tropical divergence. *J. Atmos. Sci*, **45(7)**, 1228–1251.

Takaya, K., and H. Nakamura, 2001: A formulation of a phase-independent

wave-activity flux for stationary and migratory quasigeostrophic eddies on a zonally varying basic flow. *Journal of the atmospheric sciences*, **58(6)**, 608–627.

Webster, P., 1983: The large scale structure of the tropical atmosphere. *General circulation of the atmosphere*, B. Hoskins and R. Pearce, Eds., Academic Press, 235–275.

Williamson, D. L., M. Blackburn, B. Hoskins, K. Nakajima, W. Ohfuchi, Y. O. Takahashi, Y.-Y. Hayash, H. Nakamura, M. Ishiwatari, J. McGregor, H. Borth, V. Wirth, H. Frank, P. Bechtold, N. P. Wedi, H. Tomita, M. Satoh, M. Zhao, I. M. Held, M. J. Suarez, M.-I. Lee, M. Watanabe, M. Kimoto, Y. Liu, Z. Wang, A. Molod, K. Rajendran, K. A., and R. Stratton, 2011: *The APE Atlas. NCAR/TN-484+STR.* Natilnal Center for Atmospheric Research.

Yoshioka, M., and Y. Kurihara, 2008: Influence of the equatorial warm water pool on the tropical cyclogenesis: an aqua planet experiment. *Atmospheric Science Letters*, **9(4)**, 248–254.

List of Figures

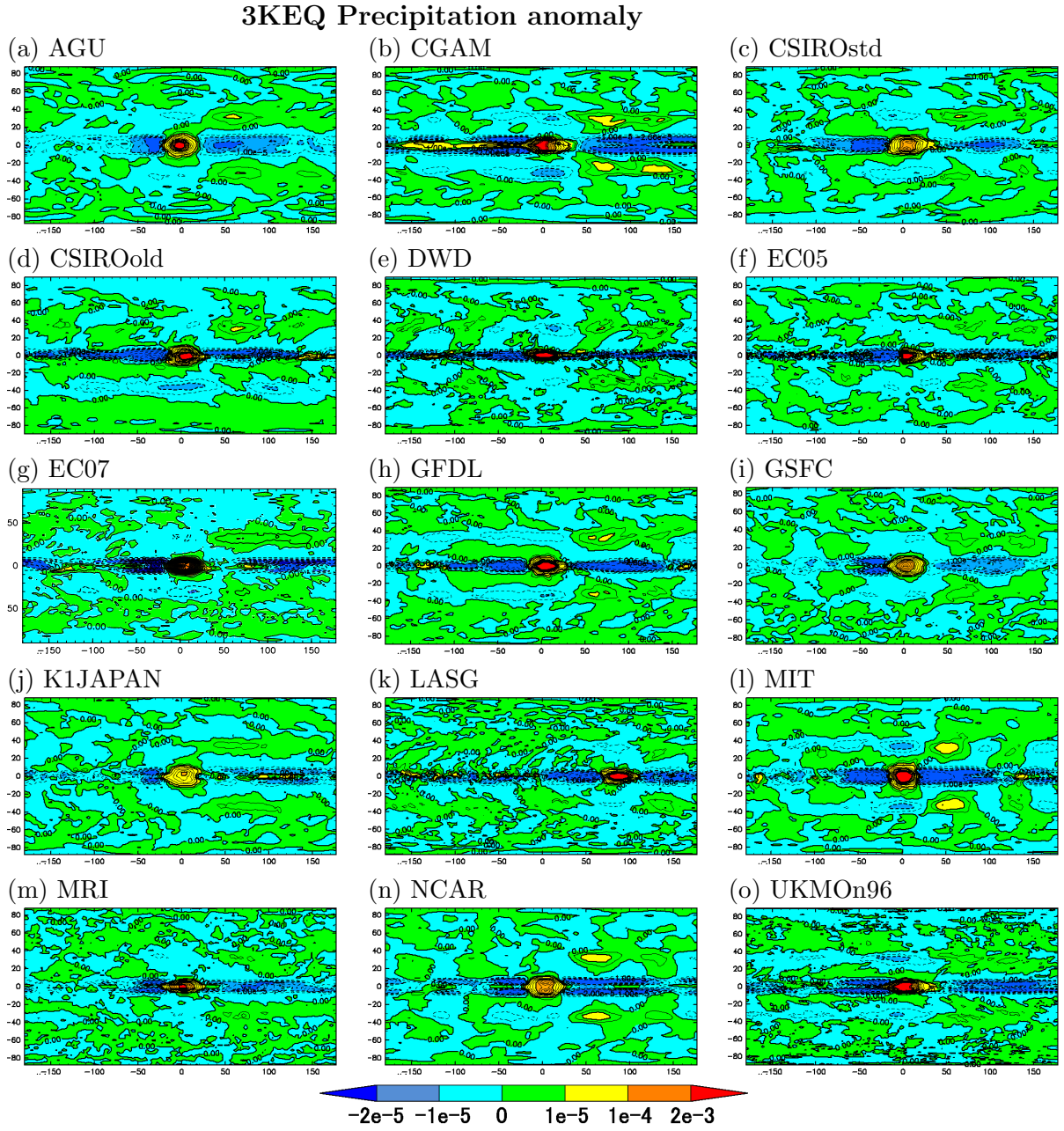

Fig. 1. Time average precipitation, 3KEQ minus the zonal average of CONTROL for individual models.

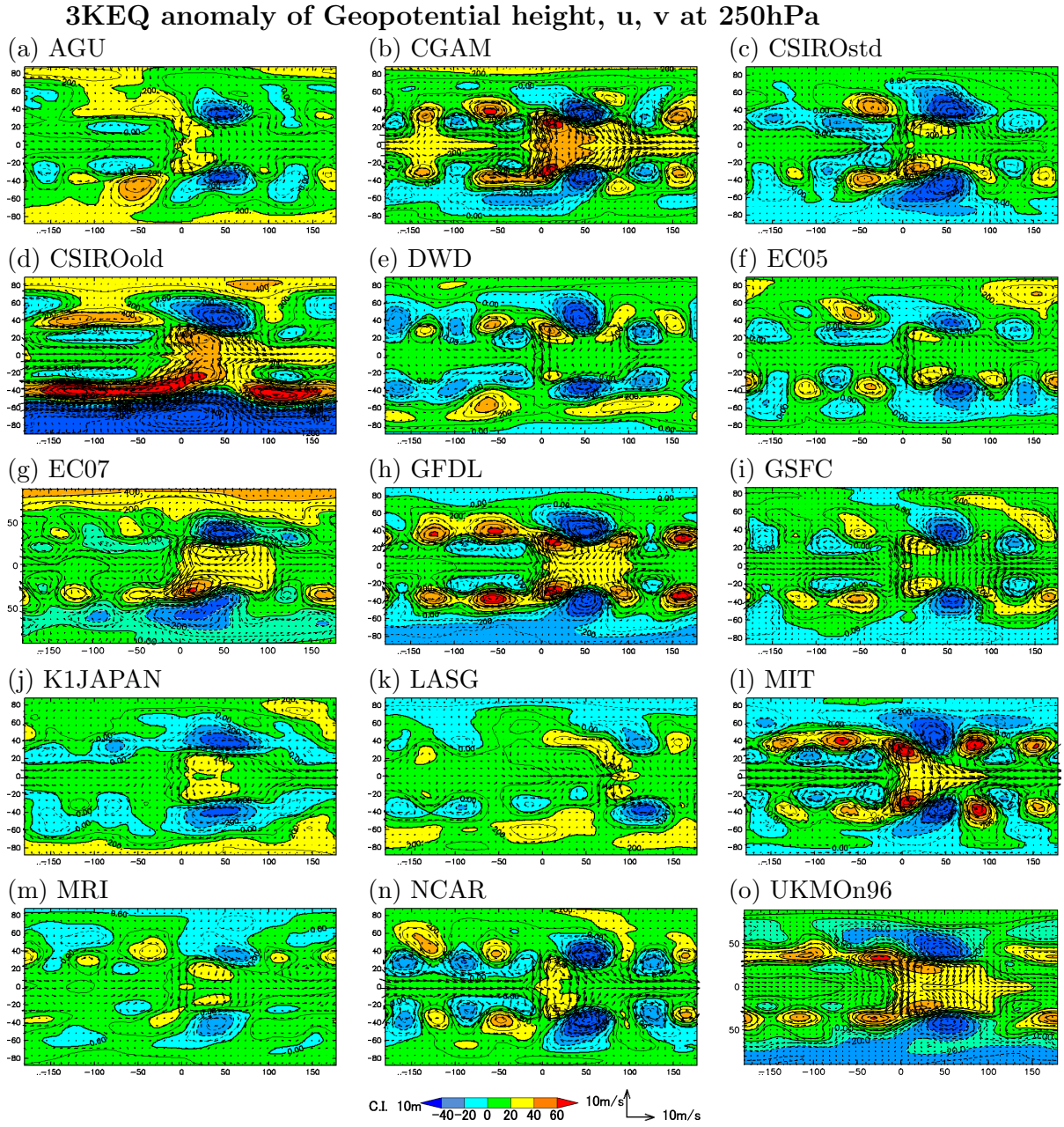

Fig. 2. Time average geopotential height and horizontal velocity vector at 250hPa, 3KEQ minus the zonal average of CONTROL for individual models.

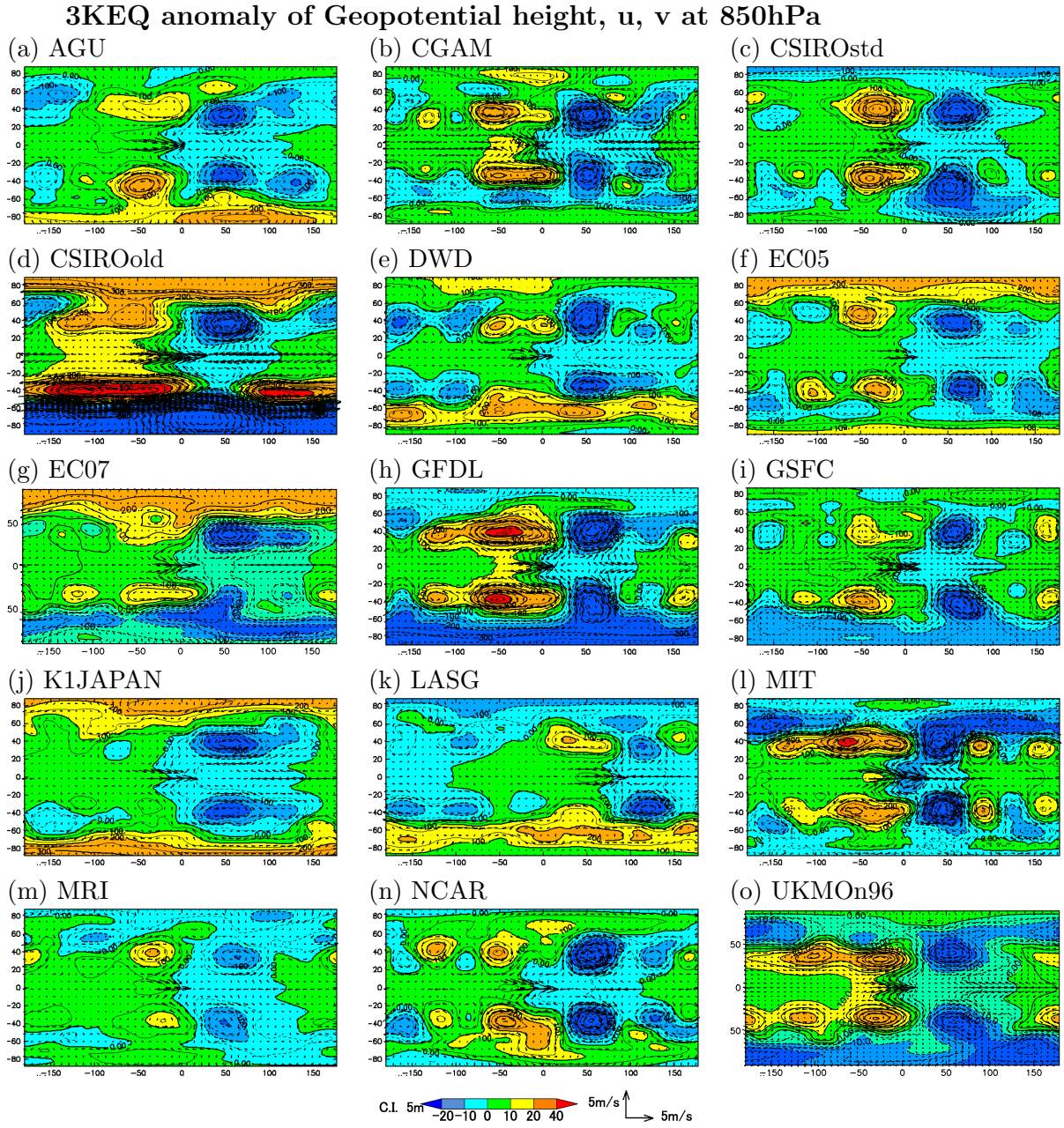

Fig. 3. Time average geopotential height and horizontal velocity vector at 850hPa, 3KEQ minus the zonal average of CONTROL for individual models.

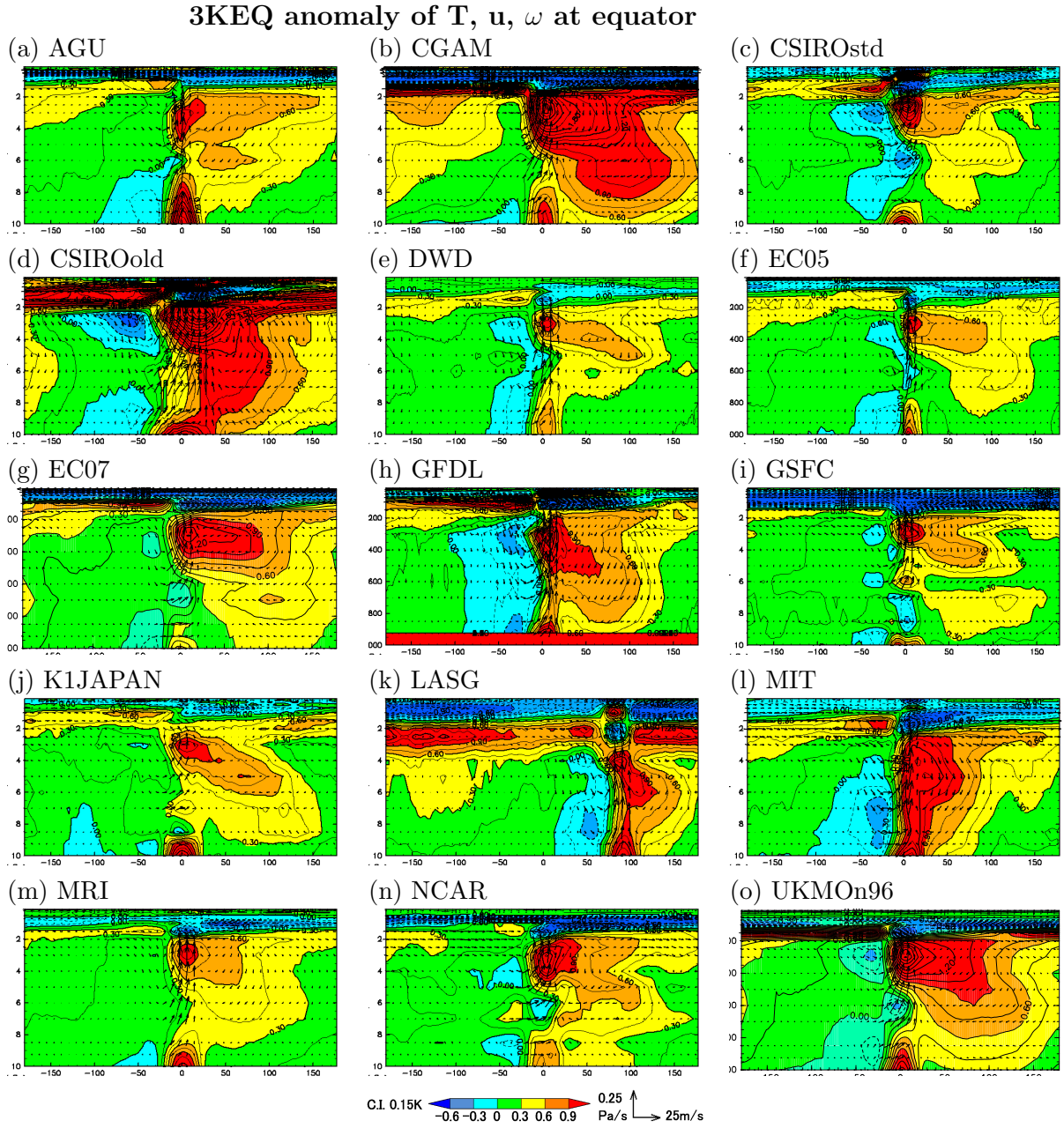

Fig. 4. Time average temperature, zonal velocity and p-velocity at the equator, 3KEQ minus the zonal average of CONTROL for individual models.

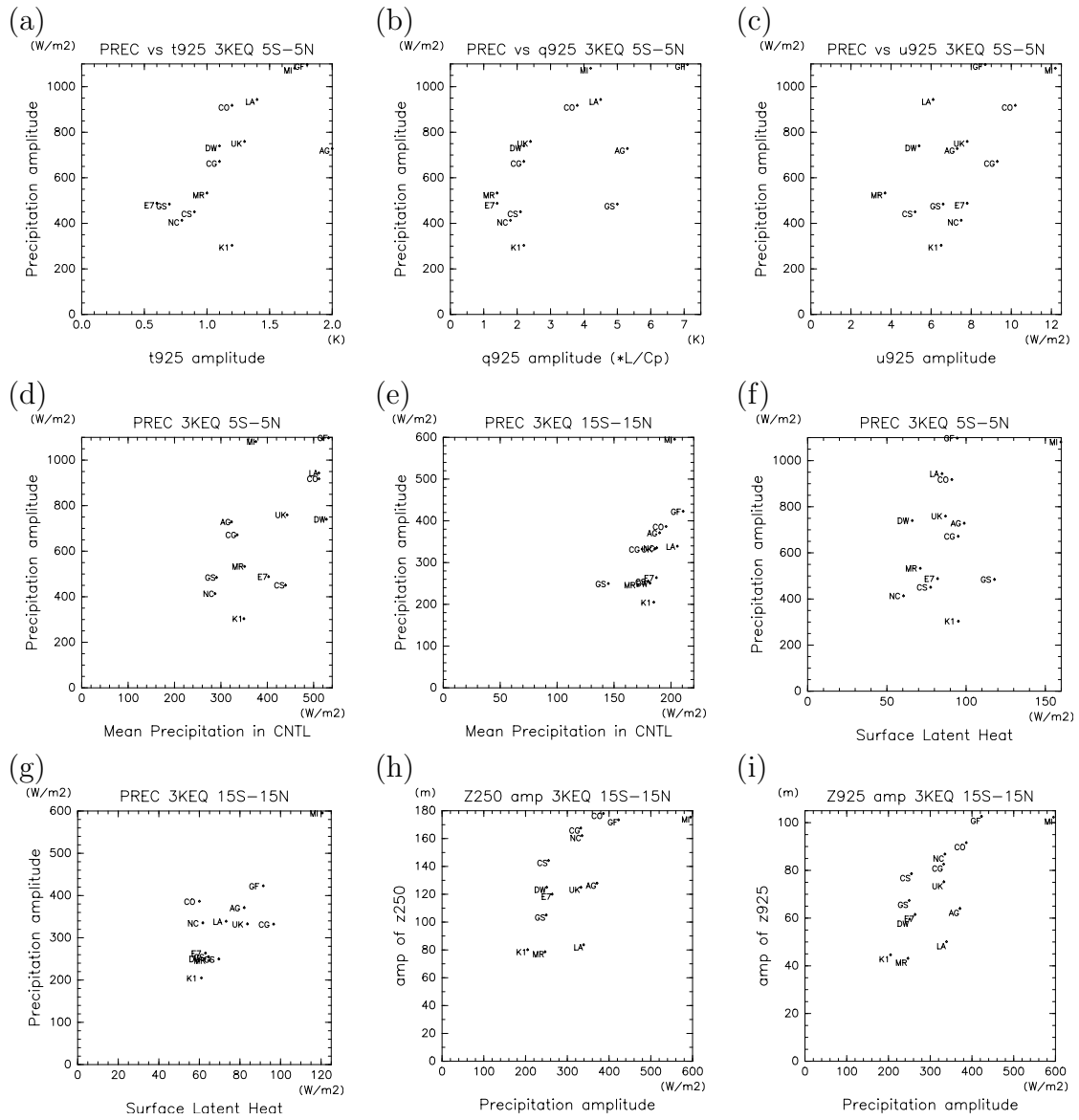

Fig. 5. Scatter plots concerning peak-to-peak amplitude of precipitation anomaly in 3KEQ: (a) peak-to-peak temperature anomaly at 925hPa vs precipitation, average within 5 degrees from the equator, (b) peak-to-peak mixing ratio anomaly at 925hP vs precipitation, average within 5 degrees from the equator, (c) peak-to-peak zonal velocity anomaly at 925hPa vs precipitation, average within 5 degrees from the equator, (d) average precipitation intencity vs amplitude of precipitation anomaly,average within 5 degrees from the equator, (e) average precipitation intencity vs amplitude of precipitation anomaly,average within 15 degrees from the equator, (f) peak-to-peak latent heat flux anomaly vs precipitation, average within 5 degrees from the equator, (g) peak-to-peak latent heat flux anomaly vs precipitation, average within 15 degrees from the equator, (h) peak-to-peak precipitation anomaly vs peak-to-peak geopotential height anomaly at 250hPa, and, (i) peak-to-peak precipitation anomaly vs peak-to-peak geopotential height anomaly at 925hPa. See Table 1 for the legends of labels.

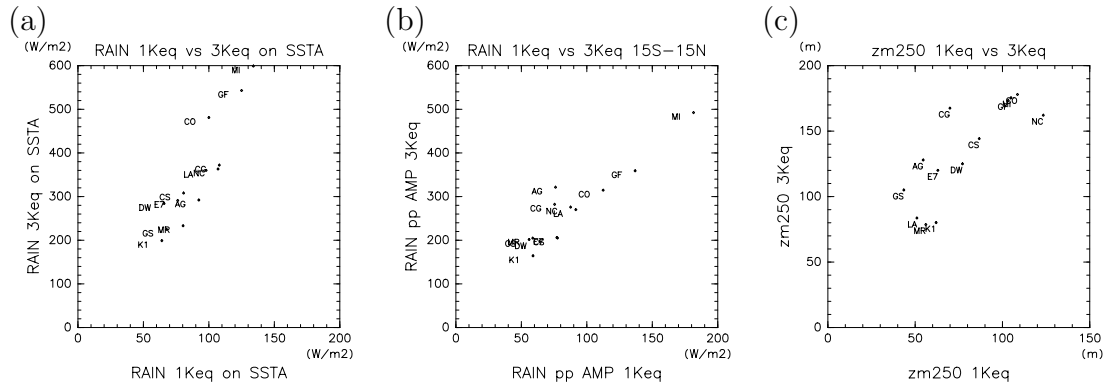

Fig. 6. Scatter plot comparing anomaly in 1KEQ and 3KEQ in the APE models. (a) Precipitation averaged over the SST anomaly. (b) Peak-to-peak amplitude of precipitation averaged within 15 degrees from the equator. (c) Peak-to-peak amplitude of mid-latitude geopotential height anomaly. See Table 1 for the legends of labels.

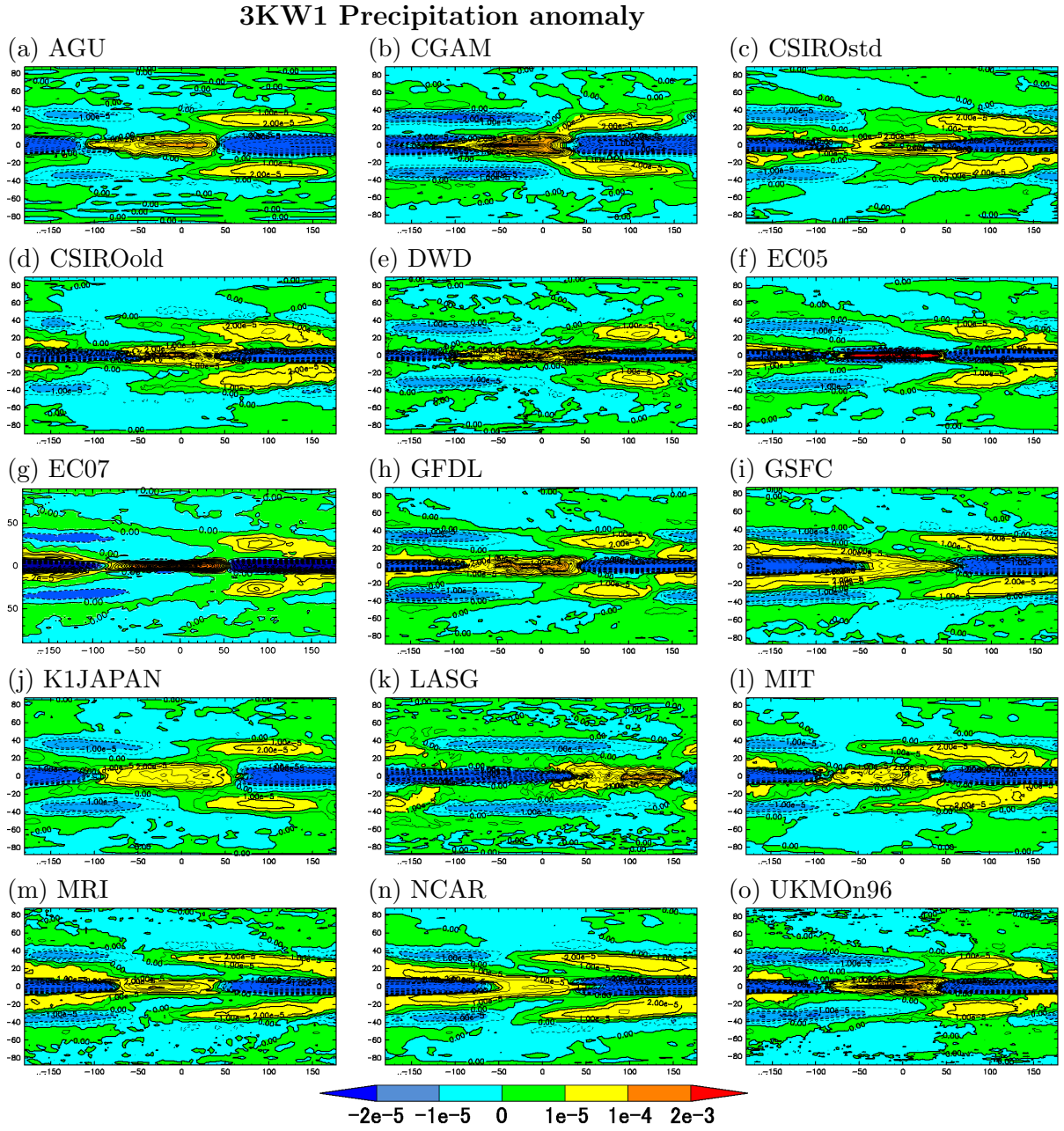

Fig. 7. Time average precipitation, 3KW1 minus the zonal average of CONTROL for individual models.

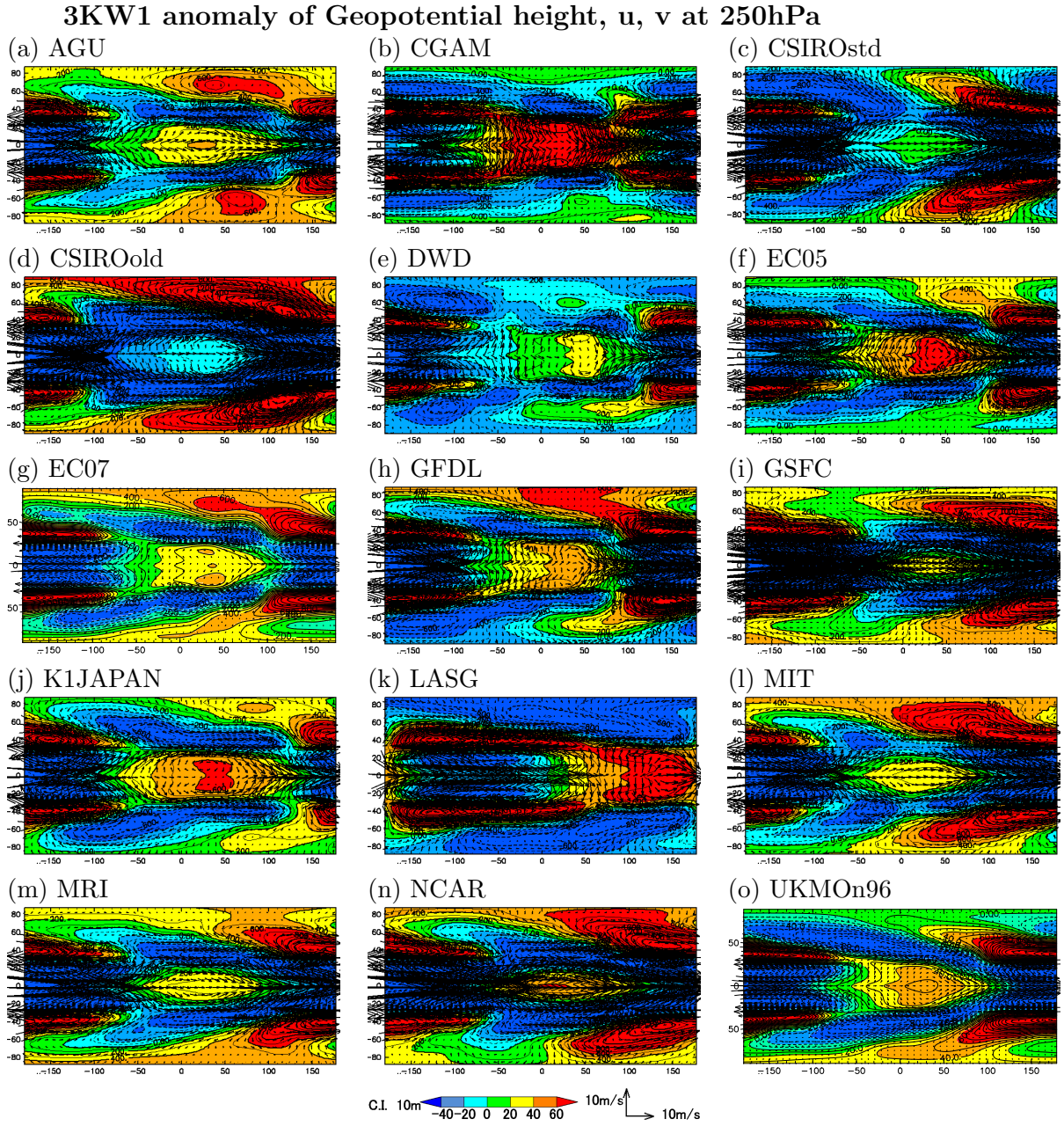

Fig. 8. Time average geopotential height and horizontal velocity vector at 250hPa, 3KW1 minus the zonal average of CONTROL for individual models.

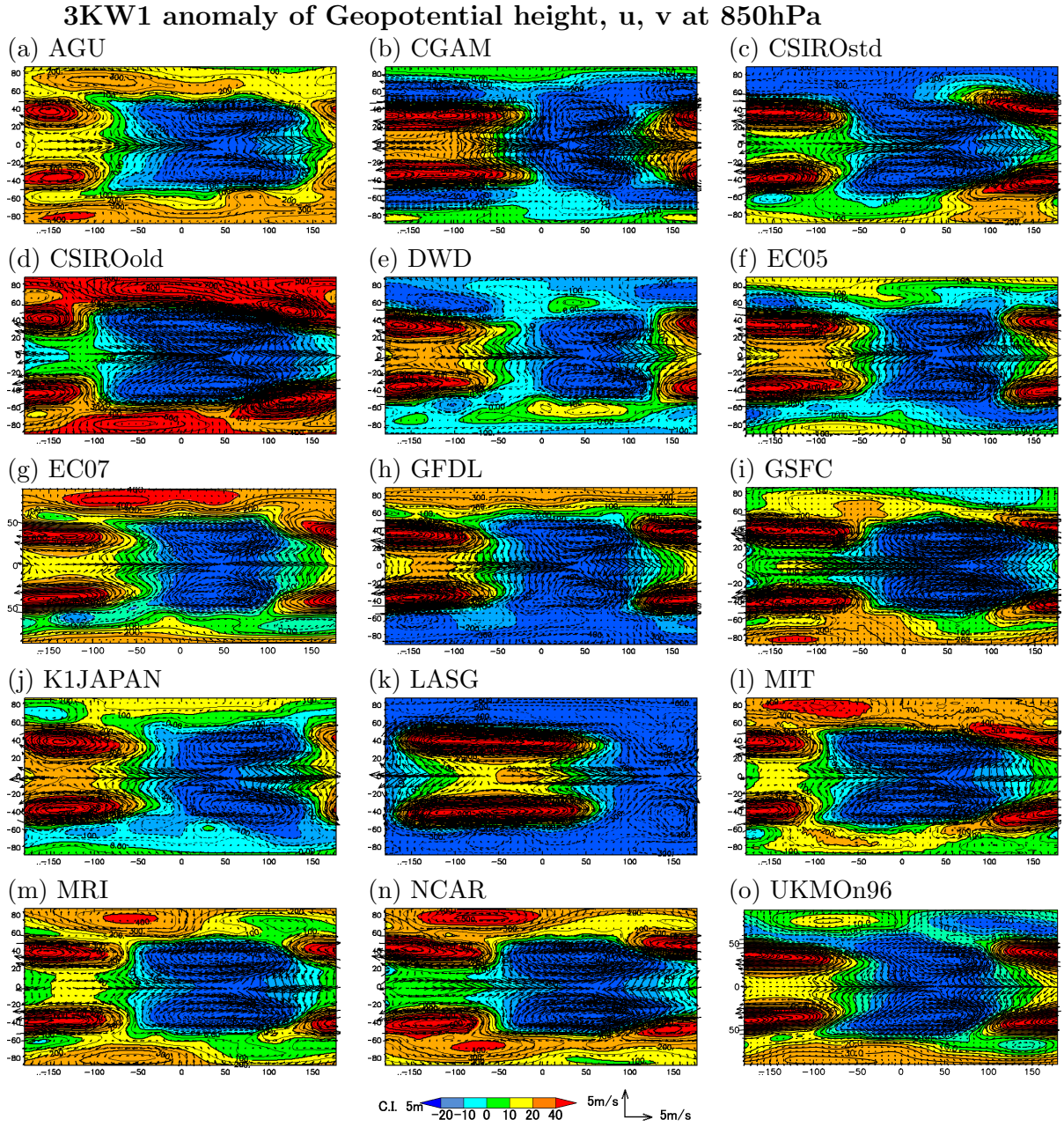

Fig. 9. Time average geopotential height and horizontal velocity vector at 850hPa, 3KW1 minus the zonal average of CONTROL for individual models.

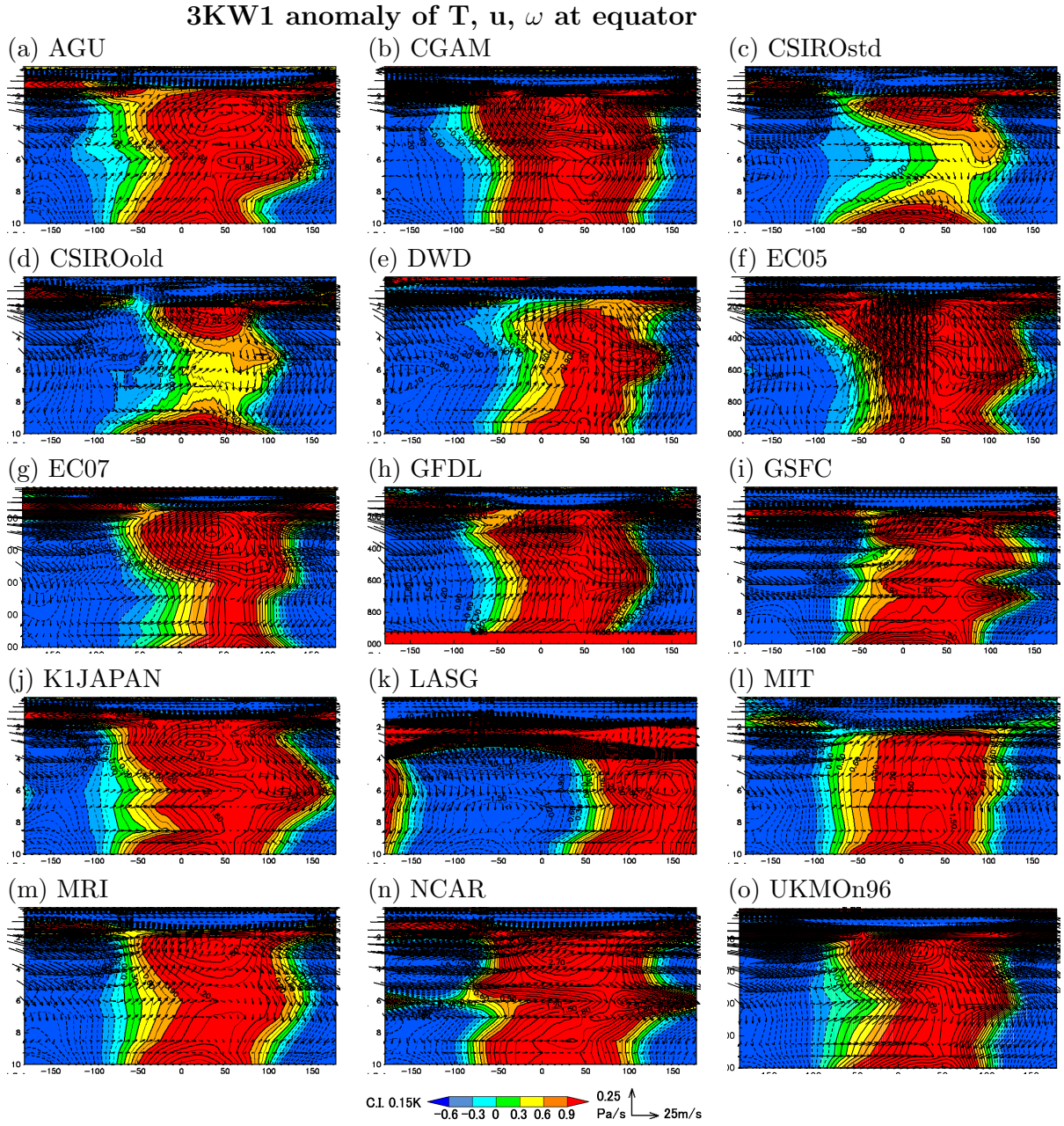

Fig. 10. Time average temperature, zonal velocity and p-velocity at the equator, 3KW1 minus the zonal average of CONTROL for individual models.

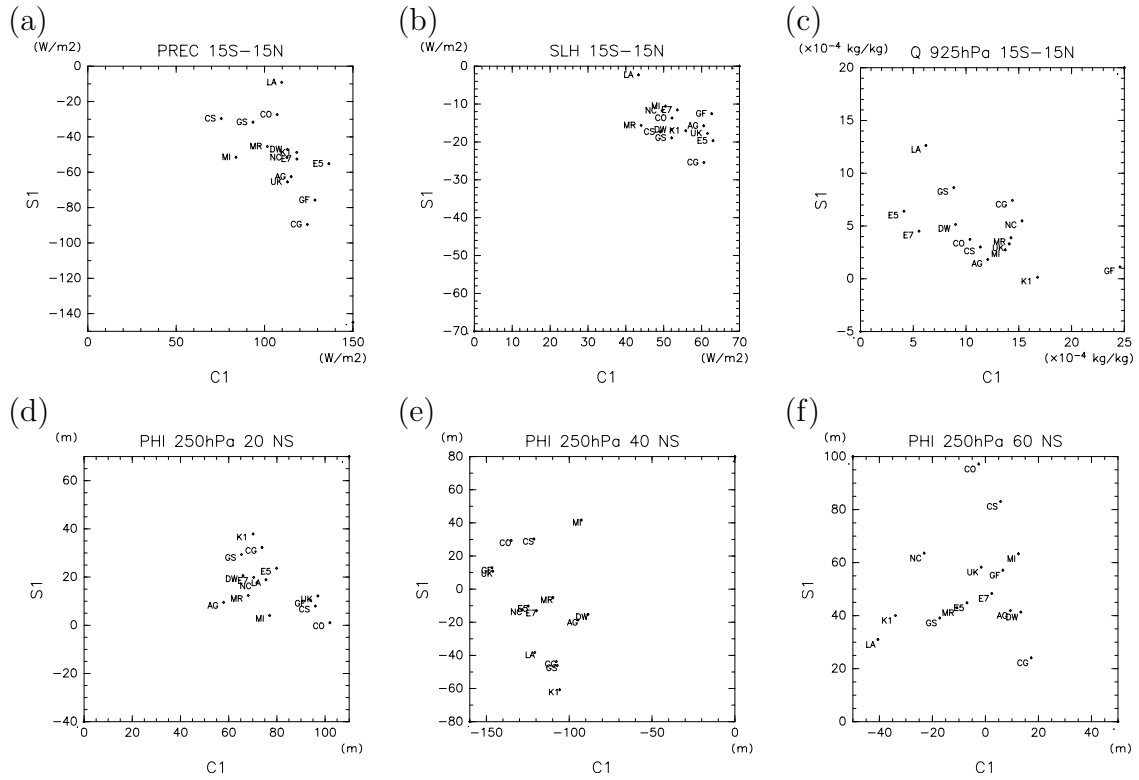

Fig. 11. Scatter plot showing sine and cosine coefficent of wave number one component in individual models. (a) precipitation averaged within 15 degrees from the equator, (b) surface latent heat flux averaged within 15 degrees from the equator, (c) mixing ration at 925hPa averaged within 15 degrees from the equator, (d) geopotential at 20 degrees latitudes, (e) geopotential at 40 degrees latitudes, and, (f) geopotential at 60 degrees latitudes. See Table 1 for the legends of labels.

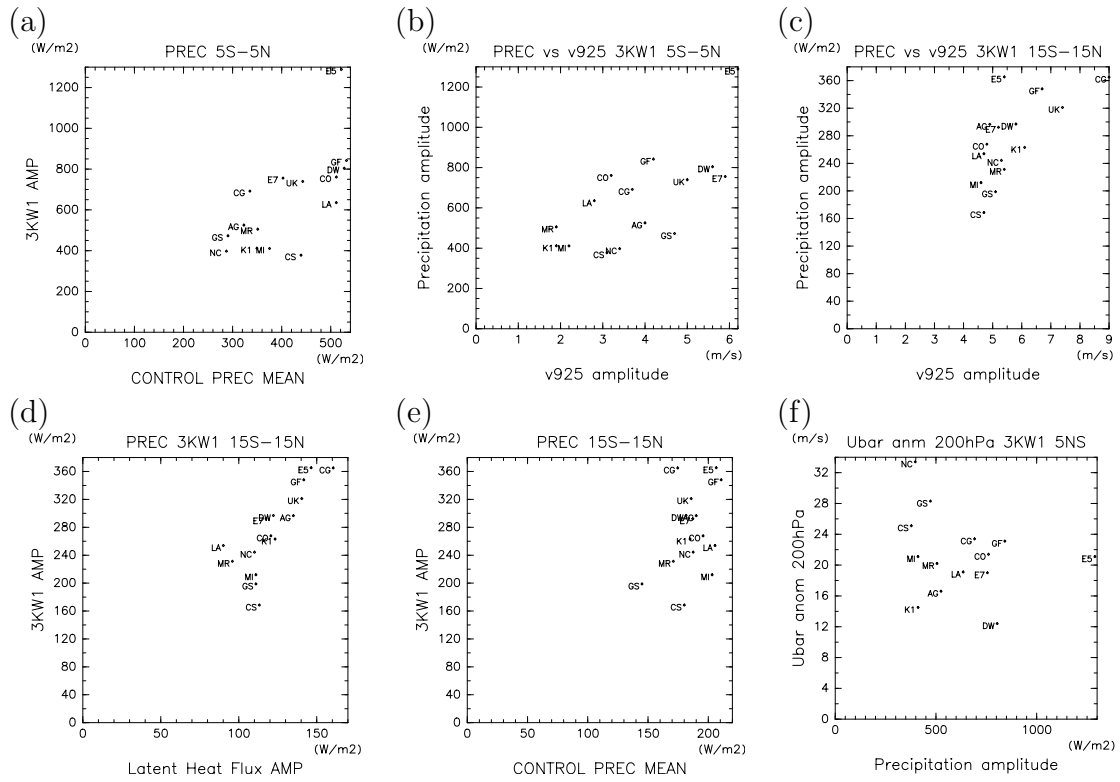

Fig. 12. Scatter plots concerning the amplitude of wavenumber one component anomaly in 3KW1 for individual models: (a) average precipitation at the equator vs precipitation at the equator, (b) meridional divergence at 925hPa vs precipitation for the average within 5 degrees from the equator, (c) meridional divergence at 925hPa vs precipitation for the average within 15 degrees from the equator, (d) surface latent heat flux vs precipitation for the average within 15 degrees from the equator, (e) mean precipitation in CONTROL vs amplitude of precipitation for the average within 15 degrees from the equator, (f) amplitude of precipitation vs zonal mean acceleration at 200hPa for the average within 15 degrees from the equator. See Table 1 for the legends of labels.

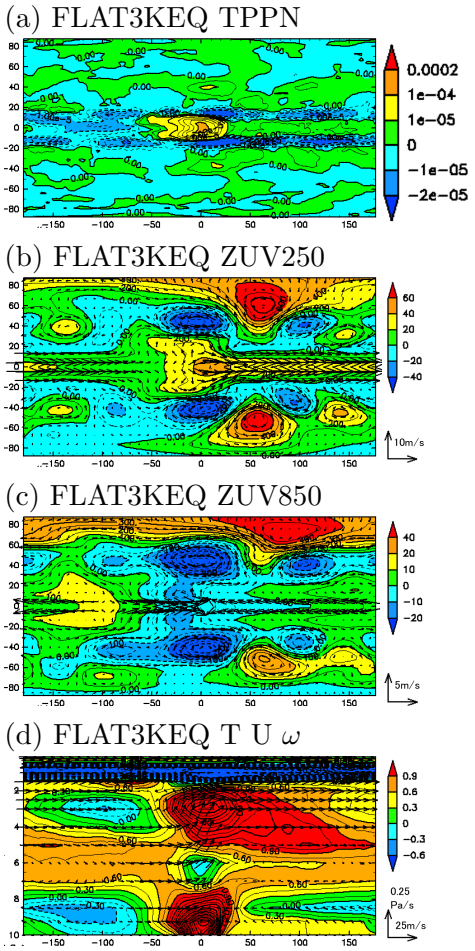

Fig. 13. Time average of FLAT3KEQ minus the zonal average of FLAT in the supplemental experiment: (a) precipitation, (b)geopotential height and horizontal wind vector at 250hPa, (c)same as (b) but for 850hPa, (d) temperature, zonal velocity and p-velocity at the equator.

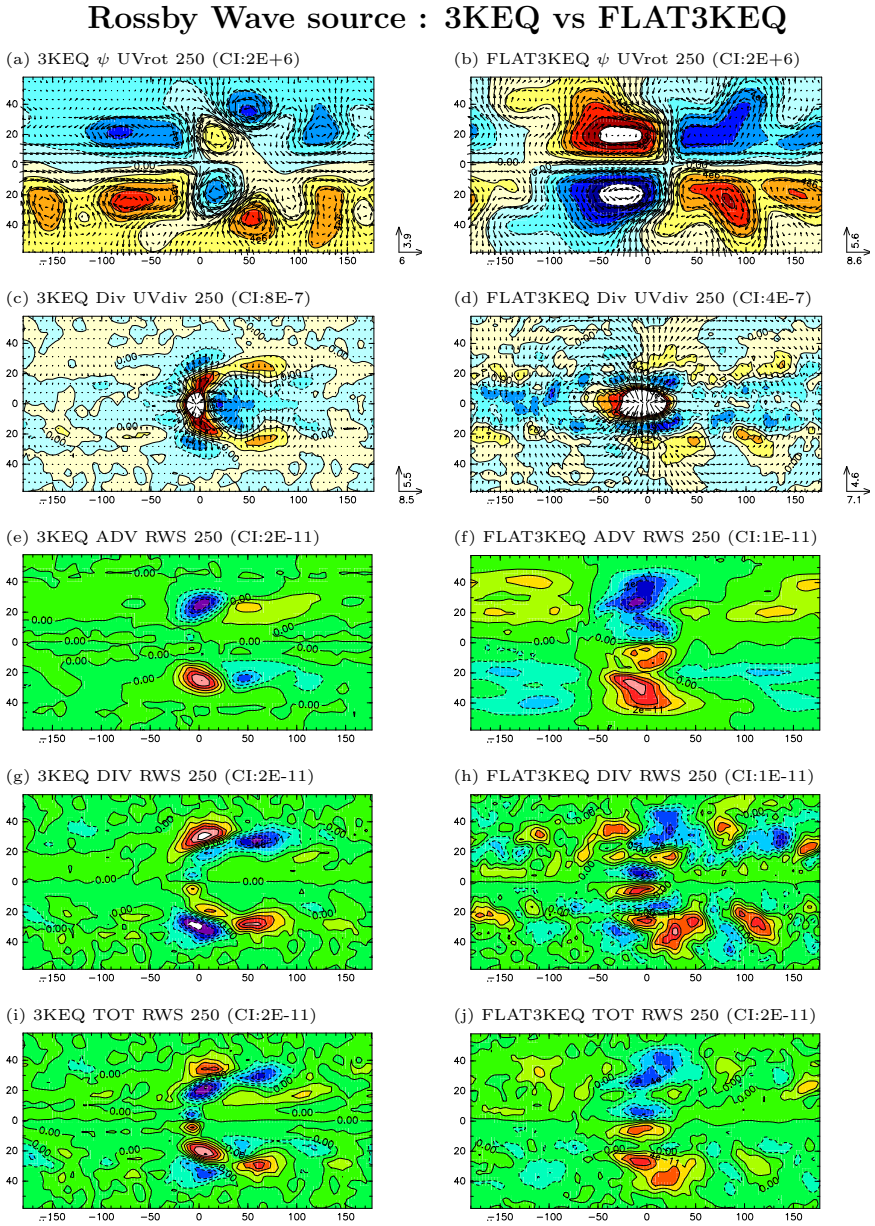

Fig. 14. Comparison between 3KEQ in AGUforAPE and FLAT3KEQ. Eddy component of stream function and rotational wind vector in 3KEQ(a) and FLAT3KEQ(b), horizontal divergence and divergent wind vector in 3KEQ(c) and FLAT3KEQ(d), advective term of Rossby wave source in 3KEQ(e) and FLAT3KEQ(f), divergent term of Rossby wave source in 3KEQ(g) and FLAT3KEQ(h), total of Rossby wave source in 3KEQ(i) and FLAT3KEQ(j),

(a)

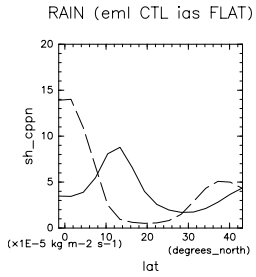

(b)

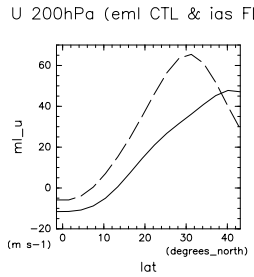

(c)

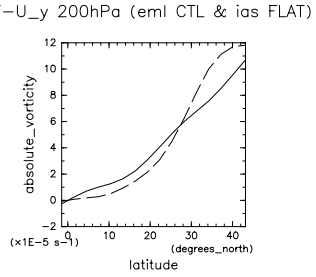

(d)

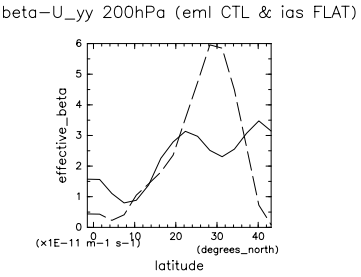

Fig. 15. Comparison of zonal average structure of upper troposphere. (a) precipitation in FLAT (solid) and 3KEQ (broken), (b) zonal wind at 200hPa in FLAT (solid) and 3KEQ (broken), (c) absolute voltivity at 200hPa in FLAT (solid) and 3KEQ (broken), and, (d) meridional gradient of absolute voltivity at 200hPa in FLAT (solid) and 3KEQ (broken).

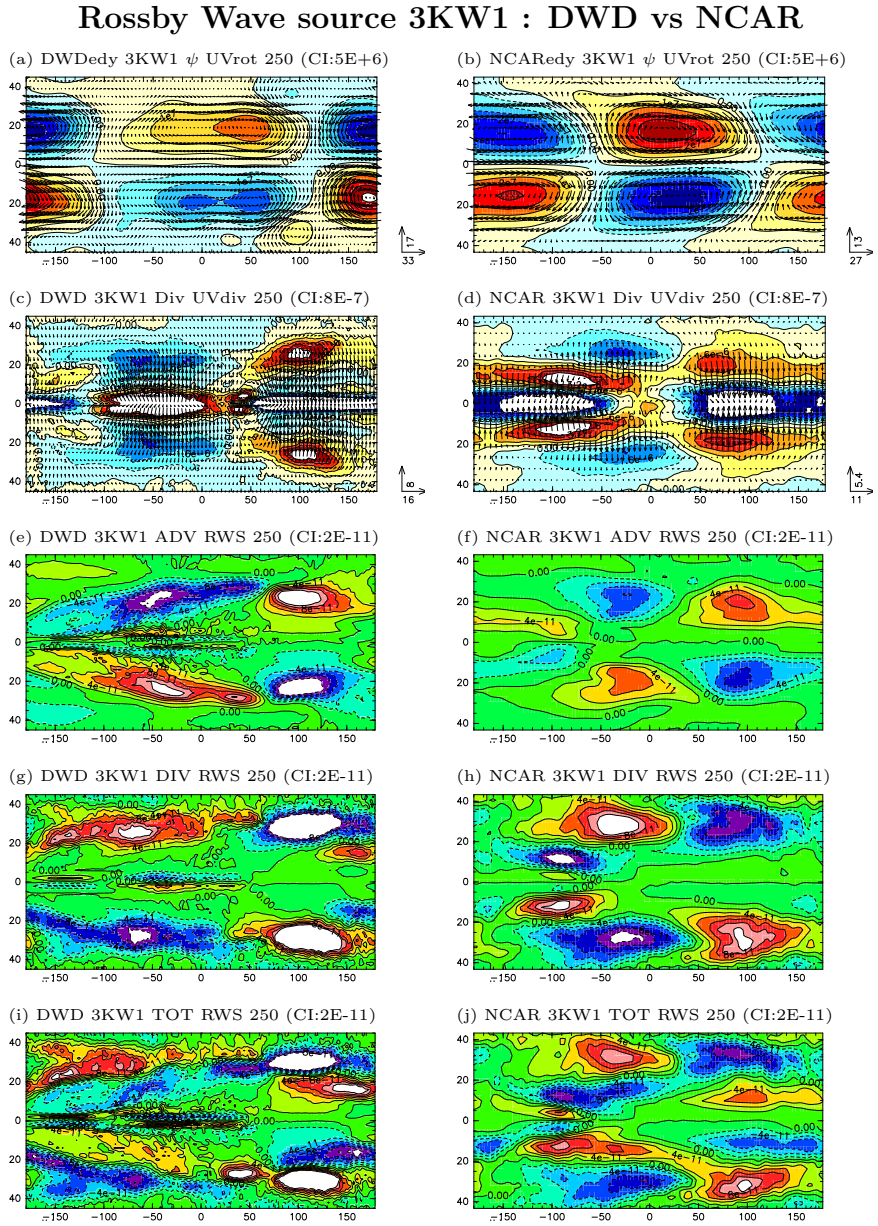

Fig. 16. Comparison between 3KEQ in DWD and 3KEQ in NCAR. Eddy component of stream function and rotational wind vector in DWD(a) and NCAR(b), horizontal divergence and divergent wind vector in DWD(c) and NCAR(d), advective term of Rossby wave source in DWD(e) and NCAR(f), divergent term of Rossby wave source in DWD(g) and NCAR(h), total of Rossby wave source in DWD(i) and NCAR(j),

List of Tables

Table 1. Participating models

GROUP SYMBOL	MODEL	HORIZONTAL RESOLUTION	NO.OF LEVELS	DEEP CONVECTION	Short symbol	note
AGU	AFES	T39	48	Emanuel	AG	
CGAM	HadAM3	3.75° x 2.5°	30	Gregory-Rawntree	CG	
CSIROstd	CCAM-05e	∼210km	18	McGregor	CS	
CSIROold	CCAM-05a	∼210km	18	McGregor	CO	
DWD	GME	∼1°	31	Tiedtke	DW	
EC05	IFS cy29r2	T159	60	Bechtold et al 2004	E5	a
EC07	IFS cy32r3	T159	60	Bechtold et al 2008	E7	
GFDL	AM2.1	2.5° x 2°	24	RAS	GF	b
GSFC	NSIPP-1	3.75° x 3°	34	RAS	GS	
K1JAPAN	CCSR/NIES 5.7	T42	20	Pan-Randall	K1	
LASG	SAMIL	R42	9	Manabe	LA	c
MIT	MIT-GCM	∼280km	40	RAS	MI	
MRI	MRI/JMA98	T42	30	Randall-Pan	MR	
NCAR	CCSM-CAM3	T42	26	Zhang-McFarlane	NC	
UKMOn96	pre-HadGAM1	1.875° x 1.25°	38	Gregory 1999	UK	

a. Western half of the 3KEQ SST anomaly is lacking.
b. Mean sea level pressure is 1000hPa.
c. Location of SST anomaly is shifted eastward by 90 degrees.